Check for
updates

On Scaling Laws for Multi-Well Nucleation Problems Without Gauge Invariances

Angkana Rüland[1] · Antonio Tribuzio[1]

Abstract

In this article, we study scaling laws for simplified multi-well nucleation problems without gauge invariances which are motivated by models for shape-memory alloys. Seeking to explore the role of the order of lamination on the energy scaling for nucleation processes, we provide scaling laws for various model problems in two and three dimensions. In particular, we discuss (optimal) scaling results in the volume and the singular perturbation parameter for settings in which the surrounding parent phase is in the first-, the second- and the third-order lamination convex hull of the wells of the nucleating phase. Furthermore, we provide a corresponding result for the setting of an infinite order laminate which arises in the context of the Tartar square. In particular, our results provide isoperimetric estimates in situations in which strong nonlocal anisotropies are present.

1 Introduction

Motivated by nucleation problems in shape-memory alloys, in this article, we study scaling laws for simplified, highly non-convex multi-well model problems with a prescribed volume constraint and with surface energy regularizations. Adopting a vari-

✉ Angkana Rüland
Angkana.Rueland@uni-heidelberg.de

Antonio Tribuzio
Antonio.Tribuzio@uni-heidelberg.de

[1] Institut für Angewandte Mathematik, Ruprecht-Karls-Universität Heidelberg, Im Neuenheimer Feld 205, 69120 Heidelberg, Germany

ational point of view and considering these results in the context of phase-transforming systems, we interpret these scaling laws as nucleation barriers for the nucleation of one phase within a matrix of the other phase. Typical systems which we have in mind are, for instance, the description of martensitic inclusions within an austenite matrix in the context of phase-transformations in shape-memory-alloys (Bhattacharya and Kohn 1997; Müller 1999). Closely related models also arise in micromagnetism and ferrofluidic droplets (Knüpfer and Nolte 2018; Knüpfer and Stantejsky 2022). Mathematically these nucleation problems correspond to isoperimetric problems in which there is a competition between a perimeter contribution and strong nonlocal anisotropies which are determined by the multi-well energies. In this article, our main objective is to contribute to an improved understanding of the complexity of possible microstructures as a consequence of the interplay between non-convexity, nonlocal anisotropy and the higher-order regularization term. In particular, we seek to identify model settings in which a relatively simple quantity, the *order of lamination* of the parent phase with respect to the nucleating phase, determines the "degree of complexity" of the scaling law for the resulting microstructure.

1.1 The Models and the General Setting

Let us describe the models which we are considering in the following sections in more detail: We study an inclusion of a phase with several variants—in the shape-memory context this would correspond to the "martensite" phase—inside a parent phase, the "austenite" phase. Following Ball (1989), Ball and James (1992) we adopt a variational perspective and consider elastic energies of the form

$$E_{el}(u) = \int_{\mathbb{R}^n} \text{dist}^2(\nabla u, K_0) dx, \quad K_0 = K \cup \{\mathbf{0}\} \subset \mathbb{R}^{n \times n} \tag{1}$$

with $n \geq 2$ and $u \in H^1(\mathbb{R}^n; \mathbb{R}^n)$. Here, physically, $u : \mathbb{R}^n \to \mathbb{R}^n$ models the deformation of the material and the set K_0 corresponds to the stress-free states at the critical temperature. We use $\mathbf{0} \in \mathbb{R}^{n \times n}$ to denote the zero matrix, which models the austenite phase. The set $K \subset \mathbb{R}^{n \times n}$ represents the variants of martensite. Seeking to provide optimal scaling laws, we simplify the problem and do not include the typical gauge invariances (e.g. invariances with respect to the action of the groups $SO(n)$ or $\text{Skew}(n)$) arising from the physical requirement of frame-indifference, but study quantitative and discrete versions of m-well problems as proposed in Ball and James (1989). Here, a main objective is the investigation of the role of the order of lamination of the parent phase with respect to the nucleating phase. More precisely, given a set $K \subset \mathbb{R}^{n \times n}$ with $\mathbf{0} \in K^{(m)} \setminus K^{(m-1)}$ for some $m \geq 1, m \in \mathbb{N}$, we seek to explore the influence of the parameter m, describing the lamination order of the parent phase with respect to the nucleating phase, on the complexity of the underlying microstructure in terms of a precise scaling law (c.f. Definition 2.1 for the definition of the lamination convex hulls $K^{(m)}$ of a set K and for the notion of a laminate of a certain prescribed order). To this end, we focus on sets $K \subset \mathbb{R}^{n \times n}$ of diagonal matrices. Moreover, we

concentrate on situations in which a suitable lamination or rank-one convex hull of K contains the zero matrix.

Following Bhattacharya and Kohn (1997), Capella and Otto (2009), Capella and Otto (2012), we express the elastic energies with the help of phase indicators which allows to decouple the gradient and the phase indicator (i.e. the projection of ∇u onto K_0). This leads to elastic energies of the following form

$$E_{el}(\chi) := \inf_{u \in H^1(\mathbb{R}^n; \mathbb{R}^n)} E_{el}(u, \chi), \quad \text{where} \quad E_{el}(u, \chi) := \int_{\mathbb{R}^n} |\nabla u - \chi|^2 dx \quad (2)$$

with $\chi \in BV(\mathbb{R}^n; K_0)$, $\chi = \mathrm{diag}(\chi_{1,1}, \ldots, \chi_{n,n})$ and $|\cdot|$ denoting the Frobenius norm.

Seeking to study the nucleation behaviour of a minority phase in a majority phase and to also include surface energies into the model, we further introduce the length scale $\epsilon > 0$ by adding to the elastic energy E_{el} a singular higher-order term of the type

$$E_{\mathrm{surf}}(\chi) := |D\chi|(\mathbb{R}^n),$$

where $|D\chi|(\mathbb{R}^n)$ denotes the total variation semi-norm of χ.

This leads to a singular perturbation problem consisting of a combination of elastic and surface energies

$$E_{\epsilon}(u, \chi) := E_{el}(u, \chi) + \epsilon E_{\mathrm{surf}}(\chi) \quad \text{and} \quad E_{\epsilon}(\chi) := E_{el}(\chi) + \epsilon E_{\mathrm{surf}}(\chi). \quad (3)$$

In this setting, it is our main objective to investigate the scaling behaviour of the minimal energy depending on the volume of the inclusion, thus providing matching upper and lower scaling bounds for the quantity

$$E_{\epsilon}(V) := \inf \left\{ E_{\epsilon}(\chi) \ : \ |\mathrm{supp}(\chi)| = V \right\}. \quad (4)$$

A key emphasis here will be on the role of the *order of lamination* of the parent phase with respect to the nucleating phase which we aim to investigate in two and three dimensions for model problems.

1.2 The Main Results

We study the scaling behaviour of the described isoperimetric problems depending on the order of lamination of the parent phase with respect to the minority phase. In what follows, we thus consider four model problems and determine the corresponding scaling laws for the nucleation of a martensitic nucleus in the austenite parent phase in the respective settings. Further possible generalizations and the role of the outlined model problems are discussed subsequently in Sect. 1.3.

1.2.1 Laminates of First Order

As the most basic example, we begin by studying the situation in which the parent phase is rank-one connected with the nucleating phase. Here we focus on two settings: In the first case, K_0 consists only of two matrices (the martensite and the austenite), while in the second case it is given by three matrices—two variants of martensite in the inclusion and one in the parent phase. In what follows we will refer to these settings as the "1+1-well" and the "2+1-well" case (and more generally the "$m+1$-well" case for $m \in \mathbb{N}$ in later parts of the article), the first slot indicating the size of the set K—and thus the number of martensitic variants—and the second slot the presence of austenite.

We begin by considering the case of two stress-free states, for which $K = \{A\}$ for some $A \in \mathrm{diag}(n, \mathbb{R})$ with $\mathrm{rank}(A) = 1$. A similar, more complex setting including a linear gauge symmetry (in the linearized theory of elasticity) had been studied in Knüpfer and Kohn (2011) where optimal scaling bounds had been deduced. Relying on the argument from Knüpfer and Kohn (2011), also in our setting, we recover the same scaling law behaviour in this situation:

Theorem 1 (Theorem 2.1, Knüpfer and Kohn 2011) *Let $E_\epsilon(V)$ be as in (4) and let $K = \{A\}$ for some $A \in diag(n, \mathbb{R})$ with $\mathrm{rank}(A) = 1$. Then there exist two positive constants $C_2 > C_1 > 0$ depending on A and n such that for every $V > 0$ and every $\epsilon > 0$ there holds*

$$C_1 r_\epsilon(V) \leq E_\epsilon(V) \leq C_2 r_\epsilon(V), \quad where \quad r_\epsilon(V) = \begin{cases} \epsilon V^{\frac{n-1}{n}} & V \leq \epsilon^n, \\ \epsilon^{\frac{n}{2n-1}} V^{\frac{2n-2}{2n-1}} & V > \epsilon^n. \end{cases}$$

We refer to the work Akramov et al. (2022) for an analogous two-dimensional result within the geometrically nonlinear theory of elasticity having full $SO(2)$ invariance.

Turning to the setting of $\#K = 2$ and imposing that the two martensitic wells are rank-one connected and that the austenite is in the lamination convex hull of K, after a change of coordinates we may without loss of generality assume that

$$K = \{A, B\}, \quad \text{with} \quad A = \begin{pmatrix} -\lambda & 0 \\ 0 & 0 \end{pmatrix}, B = \begin{pmatrix} 1-\lambda & 0 \\ 0 & 0 \end{pmatrix} \tag{5}$$

for some $\lambda \in (0, 1)$ fixed, with "austenite" given by the zero matrix (see Remark 4.4 for the details of this reduction). In this case $\mathbf{0} \in K^{(1)}$, where $K^{(1)}$ denotes the first-order lamination convex hull (and coincides with $\mathrm{conv}(K)$ in this case, see Definition 2.1 below). In contrast to the previous case in which $\#K = 1$, in the nucleation process it is now possible for the nucleating phase to form an internal microstructure lowering the elastic energy. This leads to an overall improved energy scaling behaviour in this setting for large volume fractions:

Theorem 2 *Let $E_\epsilon(V)$ be as in (4) and let K be as in (5). Then, there exist two positive constants $C_2 > C_1 > 0$ depending on K such that for every $V > 0$ and for every*

$\epsilon > 0$ *there holds*

$$C_1 r_\epsilon(V) \leq E_\epsilon(V) \leq C_2 r_\epsilon(V), \quad where \quad r_\epsilon(V) = \begin{cases} \epsilon V^{\frac{1}{2}} & V \leq \epsilon^2, \\ \epsilon^{\frac{4}{5}} V^{\frac{3}{5}} & V > \epsilon^2. \end{cases}$$

Moreover, it is possible to generalize this to arbitrary dimensions, picking up a dimensional dependence:

Corollary 1.1 *Let $E_\epsilon(V)$ be as in (4) and let $K = \{-\lambda e_1 \otimes e_1, (1-\lambda)e_1 \otimes e_1\}$ with $\lambda \in (0, 1)$ and e_1 denoting the first, normalized canonical basis vector. Then there exist two positive constants $C_2 > C_1 > 0$ depending on K and n such that for every $V > 0$ and for every $\epsilon > 0$ there holds*

$$C_1 r_\epsilon(V) \leq E_\epsilon(V) \leq C_2 r_\epsilon(V), \quad where \quad r_\epsilon(V) = \begin{cases} \epsilon V^{\frac{n-1}{n}} & V \leq \epsilon^n, \\ \epsilon^{\frac{2n}{3n-1}} V^{\frac{3n-3}{3n-1}} & V > \epsilon^n. \end{cases}$$

1.2.2 A Second-Order Laminate in Two Dimensions

Considering nucleation settings in which the parent phase is a *second-order laminate*, the elastic energy plays a stronger role in the resulting scaling law. Indeed, we expect that more microstructure is necessary in order to obey self-accommodation of the nucleus on the one hand and to ensure compatibility of the phases on the other hand. Seeking to study these effects, we consider the following set $K = \{A_1, A_2, A_3, A_4\}$ with

$$A_1 = \begin{pmatrix} -1 & 0 \\ 0 & -2 \end{pmatrix}, \ A_2 = \begin{pmatrix} -1 & 0 \\ 0 & 1 \end{pmatrix}, \ A_3 = \begin{pmatrix} 1 & 0 \\ 0 & 2 \end{pmatrix}, \ A_4 = \begin{pmatrix} 1 & 0 \\ 0 & -1 \end{pmatrix}. \tag{6}$$

In this setting, we have first- and second-order laminates given by the following formulas: $K^{(1)} := \mathrm{conv}\{A_1, A_2\} \cup \mathrm{conv}\{A_3, A_4\}$ and

$$K^{(2)} \setminus K^{(1)} = \left\{ \begin{pmatrix} \mu & 0 \\ 0 & \nu \end{pmatrix} : |\mu| < 1, |\nu| \leq 1 \right\},$$

see Fig. 1 (and where we refer to Definition 2.1 in Sect. 2.1 for the definition of the first- and second-order lamination convex hulls $K^{(1)}$ and $K^{(2)}$).

In particular, the zero matrix belongs to the lamination convex hull K^{lc} and can be obtained as

$$\frac{1}{2}\left(\frac{1}{3}A_1 + \frac{2}{3}A_2\right) + \frac{1}{2}\left(\frac{1}{3}A_3 + \frac{2}{3}A_4\right) = \mathbf{0},$$

that is the zero matrix is a second-order laminate of K.

In this setting, it turns out that indeed, the nucleation process is more expensive for large nucleation cores than in the setting of Theorem 2:

Fig. 1 The matrix set from Sect. 1.2.2: In blue the set $K^{(1)} \setminus K$, in red $K^{(2)} \setminus K^{(1)}$ (Color figure online)
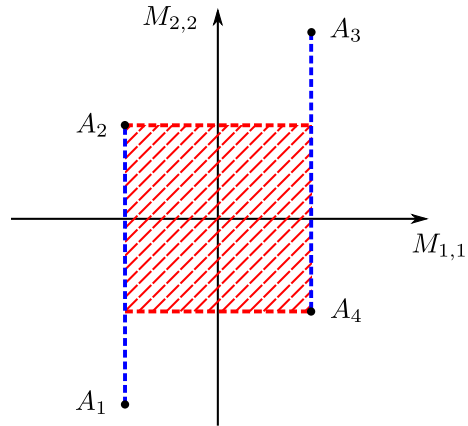
Theorem 3 *Let $E_\epsilon(V)$ be as in (4) and let K be given by the matrices in (6). Then, there exist two positive constants $C_2 > C_1 > 0$ depending on K such that for every $V > 0$ and for every $\epsilon > 0$ there holds*

$$C_1 r_\epsilon(V) \leq E_\epsilon(V) \leq C_2 r_\epsilon(V), \quad \text{where} \quad r_\epsilon(V) = \begin{cases} \epsilon V^{\frac{1}{2}} & \text{if } V \leq \epsilon^2, \\ \epsilon^{\frac{4}{7}} V^{\frac{5}{7}} & \text{if } V > \epsilon^2. \end{cases}$$

We remark that also for this setting, a higher-dimensional analogue can be obtained. Indeed, we refer to Sect. 5.3 (Proposition 5.3) in which a lower scaling bound for a second-order laminate parent phase in three dimensions is investigated. For this simple model problem we in particular recover the lower scaling bound which had earlier been derived for the cubic-to-tetragonal phase transition in the geometrically linearized theory of elasticity in Knüpfer et al. (2013) (with gauge group $Skew(3)$). As a consequence, in spite of our substantial simplification in ignoring gauges, these models may capture some of the mathematical features of physically more realistic models and can mathematically thus be regarded as interesting, simpler substitutes for these which may allow for a more detailed analysis.

1.2.3 A Three-Dimensional Third-Order Laminate

In addition to the two-dimensional settings, we also consider a three-dimensional problem for which the zero matrix is a third-order laminate. To this end, we consider the set of wells given by

$$K = \left\{ \begin{pmatrix} 2 & 0 & 0 \\ 0 & -2 & 0 \\ 0 & 0 & 1 \end{pmatrix}, \begin{pmatrix} -2 & 0 & 0 \\ 0 & -2 & 0 \\ 0 & 0 & 1 \end{pmatrix}, \begin{pmatrix} -3 & 0 & 0 \\ 0 & 2 & 0 \\ 0 & 0 & 1 \end{pmatrix}, \begin{pmatrix} 3 & 0 & 0 \\ 0 & 2 & 0 \\ 0 & 0 & 1 \end{pmatrix}, \right.$$
$$\left. \begin{pmatrix} 1 & 0 & 0 \\ 0 & -1 & 0 \\ 0 & 0 & -1 \end{pmatrix}, \begin{pmatrix} -1 & 0 & 0 \\ 0 & -1 & 0 \\ 0 & 0 & -1 \end{pmatrix}, \begin{pmatrix} -4 & 0 & 0 \\ 0 & 1 & 0 \\ 0 & 0 & -1 \end{pmatrix}, \begin{pmatrix} 4 & 0 & 0 \\ 0 & 1 & 0 \\ 0 & 0 & -1 \end{pmatrix} \right\}, \tag{7}$$

Fig. 2 The matrix set from
Sect. 1.2.3: In blue the set
$K^{(1)} \setminus K$, in red $K^{(2)} \setminus K^{(1)}$, in
green $K^{(3)} \setminus K^{(2)}$
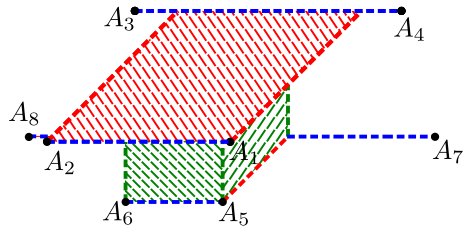
see also Fig. 2. For this choice of the set K the lamination convex hull $K^{(lc)}$ contains matrices with lamination orders up to order three. In particular, the zero matrix has lamination order three.

In this setting, we consider lower scaling bounds and show that again these are determined by the order of lamination:

Proposition 1.2 *Let $E_\epsilon(V)$ be as in* (4) *and let K be as* (7). *Then, there exists a positive constant $C > 0$ depending on K such that for every $V > 0$ and for every $\epsilon > 0$ it holds*

$$E_\epsilon(V) \geq Cr_\epsilon(V), \quad where \quad r_\epsilon(V) = \begin{cases} \epsilon V^{\frac{2}{3}}, & V \leq \epsilon^3, \\ \epsilon^{\frac{3}{7}} V^{\frac{6}{7}}, & V > \epsilon^3. \end{cases}$$

We expect that matching upper bounds could be proved using the three-dimensional construction from Rüland and Tribuzio (2021, Proposition 6.3). As this however is technically rather involved due to the presence of the higher order of lamination and the necessity of achieving compatibility with the parent phase at the boundary of the inclusion domain in all three directions, we do not provide the matching upper bounds here but postpone this to future work.

1.2.4 A Laminate of Infinite Order

Last but not least, we study a setting which is "almost rigid" in that the zero matrix is an infinite order laminate of the nucleating phases. Here, the set K consists of the matrices forming the Tartar square (Aumann and Hart 1986; Casadio-Tarabusi 1993; Nesi and Milton 1991; Scheffer 1975; Tartar 1993), i.e. they are given by $K = \{A_1, A_2, A_3, A_4\} \subset \mathbb{R}^{2\times 2}$ with

$$A_1 = \begin{pmatrix} -1 & 0 \\ 0 & -3 \end{pmatrix}, \ A_2 = \begin{pmatrix} -3 & 0 \\ 0 & 1 \end{pmatrix}, \ A_3 = \begin{pmatrix} 1 & 0 \\ 0 & 3 \end{pmatrix}, \ A_4 = \begin{pmatrix} 3 & 0 \\ 0 & -1 \end{pmatrix}. \tag{8}$$

In this setting, very complicated microstructure has to emerge in order to ensure self-accommodation and compatibility. Hence, the infinite order of lamination is reflected in a very rigid, high energy scaling law behaviour:

Theorem 4 *Let $E_\epsilon(V)$ be as in* (4) *and let K consist of the matrices in* (8). *Then, there exist four positive constants $C^{(1)} > C^{(2)} > 0$, $C_2 > C_1 > 0$ depending on K such that for every $V > 0$ and for every $\epsilon > 0$ there holds*

$$C_1 r_\epsilon^{(1)}(V) \le E_\epsilon(V) \le C_2 r_\epsilon^{(2)}(V), \text{ where } r_\epsilon^{(j)}(V) = \begin{cases} \epsilon V^{\frac{1}{2}} & \text{if } V \le \epsilon^2, \\ V \exp\left(-C^{(j)}\left(\log\left(\frac{V}{\epsilon^2}\right)\right)^{\frac{1}{2}}\right) & \text{if } V > \epsilon^2. \end{cases}$$

The nucleation result of Theorem 4 is in parallel to the scaling law from Rüland and Tribuzio (2022) and the earlier upper bound estimates from Chipot (1999) and Winter (1997) in which the scaling behaviour of a singular perturbation problem for the Tartar square was analyzed in a *fixed* domain with Dirichlet boundary conditions. In both the fixed domain and the nucleation setting, a rather unusual "high energy" behaviour is deduced in the scaling law. In the fixed domain setting this is manifested in a *subalgebraic* scaling law behaviour in the singular perturbation parameter ϵ, i.e. in a scaling law behaviour which is slower (as $\epsilon \to 0$) than any power law behaviour. In the nucleation problem this is reflected in the large volume bound which only deviates from the linear volume scaling by a *subalgebraic* volume correction term. In this sense, the nucleation problem is "rather close to being incompatible". We remark that while our result quantitatively captures this major "footprint" of the infinite order of lamination, it does not provide sharp values for the constants $C^{(j)}$, encoding the *detailed* subalgebraic behaviour. We refer to Sect. 7 for a more detailed discussion on this.

1.3 Generalizations

The results from Sects. 1.2.1–1.2.4 illustrate the relevance of the order of lamination of the parent phase with respect to the nucleating phase. We emphasize that in our presentation we have selected prototypical model settings for the sets K. These are chosen in such a way that the zero matrix is in the corresponding generalized convex hull (e.g. the first, second, third lamination or rank-one convex hull) and that additionally a certain "nonlinear structural condition" is present. The latter is a central ingredient in our derivation of the lower scaling bounds by means of commutator estimates which allow us to iteratively obtain improved control of the a priori possible Fourier-space concentration of the phase indicators.

This is ensured by the property that the diagonal components of the phase indicator "determine" each other in a way which reflects the order of lamination. This is particularly visible for the Tartar square. Due to the absence of rank-one connections, in this setting each diagonal component already determines the other diagonal component. In the case of the differential inclusion $\nabla u \in \{A_1, \ldots, A_4\}$, together with the diagonal structure of the matrices A_j, this already implies the qualitative rigidity of the Tartar square (see Müller 1999; Rüland and Tribuzio 2022, Section 3.1) which is made quantitative in Rüland and Tribuzio (2022).

For situations in which rank-one directions between the wells are present, the "nonlinear structural condition" is only valid in a weaker form with not all diagonal components "determining" each other. Here, there is a hierarchy of nonlinear relations: Only some diagonal components determine some of the other components, e.g. in our example from Sect. 1.2.2 only the second diagonal component $\chi_{2,2}$ determines the first

component $\chi_{1,1}$ but not conversely. In the examples of sets $K \subset \text{diag}(n, \mathbb{R})$ which are discussed in this article the structure of the wells is chosen exactly in such a way that the number and structure of the nonlinear relations corresponds to the order of lamination of the parent phase. In this sense, in these cases the order of lamination determines the scaling behaviour of the nucleation problem. In particular, we emphasize that our specific examples are only exemplary model choices of settings in which this idea can be used and many more settings could be analysed with this method.

Building on these ideas for the lower scaling bounds and formally computing the associated optimization problems similarly as outlined in the following sections, we further conjecture that it is possible to produce wells $K \subset \text{diag}(n, \mathbb{R})$ with nucleation scaling behaviour of the order

$$C_1 r_\epsilon(V) \leq E_\epsilon(V) \leq C_2 r_\epsilon(V), \quad \text{where} \quad r_\epsilon(V) = \begin{cases} \epsilon V^{\frac{n-1}{n}} & \text{if } V \leq \epsilon^n, \\ \epsilon^{\frac{2n}{n^2+2n-1}} V^{\frac{n^2+2n-3}{n^2+2n-1}} & \text{if } V > \epsilon^n, \end{cases} \tag{9}$$

in n-dimensional situations for constants $0 < C_1 \leq C_2$. In particular, this "interpolates" between the rather low energy $2 + 1$-well case and the very rigid, energetically expensive Tartar setting.

Remark 1.3 (*On the role of the order of lamination*) In the examples from Theorems 2 and 3, Corollary 1.1 and Propositions 1.2 and 5.3, the role of the order of lamination of the parent phase with respect to the nucleating phase is directly reflected in the associated (lower) scaling bounds. Indeed, in all these examples, the (lower) scaling bounds are given in terms of the following estimate relating the dimension $n \in \mathbb{N}$ and the lamination order $m \in \mathbb{N}$

$$E_\epsilon(V) \geq C r_\epsilon(V), \quad \text{where} \quad r_\epsilon(V) = \begin{cases} \epsilon V^{\frac{n-1}{n}}, & V \leq \epsilon^n, \\ \epsilon^{\frac{2n}{n(m+2)-1}} V^{\frac{n(m+2)-3}{n(m+2)-1}}, & V > \epsilon^n, \end{cases} \tag{10}$$

for some constant $C > 0$. In parts (e.g. in our two-dimensional results) even corresponding matching upper bounds are proved in our discussion below. Moreover, also the example from Knüpfer et al. (2013) and our conjectured scaling bounds from (9) fit into this scheme (with $n = 3$, $m = 2$ and with $n = n$, $m = n$, respectively).

Let us emphasize that this (lower) scaling bound behaviour is no coincidence: Indeed, as explained in the above discussion on the general structure of our sets K, the sets K are chosen in such a way that a certain nonlinear structure is present allowing for an iterative application of the commutator arguments from Rüland and Tribuzio (2021). More precisely, all our sets K from above are such that the number of iterations of these commutator estimates is directly related to the order of lamination of the parent phase with respect to the nucleating phase. Thus, by carrying out the optimization arguments from below, this eventually leads to the (lower) scaling bounds stated in (10).

In addition to the discussion from Remark 1.3, let us however also caution that, in general, the lamination order of the parent phase with respect to the nucleating

phase certainly is *not* the only factor determining the scaling behaviour in nucleation problems. Indeed, considering for instance sets K giving rise to two-dimensional "stair-case laminates" as in Conti et al. (2005), it is possible to create arbitrarily high orders of lamination. In this situation it is however not expected that this is necessarily reflected in the nucleation scaling law. We postpone more detailed results on this to future work.

1.4 Relation to the Literature

The results derived in this article mathematically fall into the class of isoperimetric inequalities (Maggi 2012) in which anisotropies are present. Due to the presence of the strong anisotropies, for large volumes, balls are in general no longer minimizers of these isoperimetric problems, but interesting microstructure emerges as a competition between the anisotropic nonlocal and the surface energies. These questions arise naturally in nucleation processes in materials science. In the context of shape-memory alloys, these have, for instance, been studied for the incompatible two-well problem (Chaudhuri and Müller 2004), for the cubic-to-tetragonal phase transformation in the geometrically linearized theory of elasticity (Knüpfer et al. 2013), for the geometrically linearized two-well problem (Knüpfer and Kohn 2011) and the boundary nucleation for the cubic-to-tetragonal phase transformation (Bella and Goldman 2015). The location of nucleation was also studied in Ball and Koumatos (2016). In the absence of self-accommodation bounds have been deduced for the cubic-to-tetragonal phase transformation in Knüpfer and Otto (2019). Moreover, special constructions and behaviour is known in highly symmetric situations in two dimensions (Cesana et al. 2020; Conti et al. 2017b).

Many of these results and ideas are closely related to singular perturbation problems for shape-memory materials with prescribed boundary conditions (see for instance, Chan and Conti 2014, 2015; Conti et al. 2020, 2017a; Chipot and Müller 1999; Capella and Otto 2009, 2012; Conti 2000; Conti and Zwicknagl 2016; Kohn and Müller 1992, 1994; Lorent 2001, 2006; Rüland and Tribuzio 2021, 2022; Rüland 2016) and the use of scaling as a selection mechanism for wild microstructure (Rüland et al. 2018a, b). Although in spirit similar to these singular perturbation problems, due to the *flexibility* of the *domain geometry*, in the nucleation setting the problem is less constrained and has more freedom to relax, in part leading to interesting new behaviour.

We emphasize that related questions and results have also been considered in other physical systems such as in compliance minimization (Kohn and Wirth 2014, 2016), micromagnetism (Choksi et al. 1999) or in models motivated by Coulombic interactions with radially symmetric nonlocal contributions (Knüpfer and Muratov 2013; Muratov and Knüpfer 2014).

1.5 Outline of the Article

The remainder of the article is structured as follows: After briefly recalling a number of auxiliary results in Sect. 2, we deal with the scaling laws from Sects. 1.2.1–1.2.4 in individual sections splitting the proofs into lower bound estimates and upper bound

constructions. Thus, in Sect. 3 we begin by recalling the result from (Knüpfer and Kohn 2011) and illustrating how the method from Knüpfer and Kohn (2011) yields the behaviour of the 1+1 well case. In Sect. 4 we invoke Fourier tools to deduce improved lower bounds and complement these with matching upper bounds leading to the proof of Theorem 2. Building on these ideas, in Sect. 5 we discuss second-order laminates in two and three dimensions. In three dimensions we in particular recover the lower scaling bound from Knüpfer et al. (2013) in our model problem (see Proposition 5.3). In Sect. 6 we then show that the lower bound estimates are robust and can also be applied to deduce bounds for third-order laminates in three dimensions which results in the proof of Proposition 1.2. In Sect. 7 we then deduce scaling bounds for infinite order laminates for the Tartar square. Finally, we conclude the article in Sect. 8 by briefly summarizing our main findings and giving a short outlook.

2 Preliminary Results

In this section we collect some intermediate results that will be used in the following sections. Although we mainly treat two- and three-dimensional problems, presenting the results of this section in their general version requires no additional effort.

Here and in what follows, when writing $a \sim b$ we mean that $c^{-1}a \leq b \leq ca$ for some constant $c > 0$ independent of ϵ and V. Analogously we will write $a \lesssim b$ and $a \gtrsim b$ meaning $a \leq cb$ and $a \geq cb$, respectively.

2.1 Laminates and Lamination Convex Hulls

Due to its relevance for our arguments, we recall the notion of the lamination convex hull of a compact set $K \subset \mathbb{R}^{n \times n}$.

Definition 2.1 (Lamination convex hull) Let $K \subset \mathbb{R}^{n \times n}$ be a compact set. Iteratively, we define the following lamination convex hulls

$$K^{(0)} := K,$$
$$K^{(m)} := \{M \in \mathbb{R}^{n \times n} : M = \lambda A + (1 - \lambda)B \text{ for } A, B \in K^{(m-1)}, \ \lambda \in [0, 1]\} \text{ for } m \geq 1.$$

An element in $K^{(m)} \setminus K^{(m-1)}$ is called a *laminate of order m*. The *lamination convex hull of K* is defined as

$$K^{(lc)} := \bigcup_{m=0}^{\infty} K^{(m)}.$$

2.2 Normalization

In considering and estimating our energies which a priori depend on the two parameters ϵ and V, we can always reduce ourselves to a one-parameter problem by a normalization argument. Let E_ϵ be as in (3) and let $u \in H^1(\mathbb{R}^n; \mathbb{R}^n)$, $\chi \in BV(\mathbb{R}^n; K_0)$ be

given, where $K_0 = K \cup \{\mathbf{0}\} \subset \mathbb{R}^{n \times n}$ and $K \subset \mathbb{R}^{n \times n}$ is a discrete set. By setting $u_\epsilon(x) := \epsilon^{-1} u(\epsilon x)$, $\chi_\epsilon(x) := \chi(\epsilon x)$, we obtain

$$E_\epsilon(u, \chi) = \epsilon^n E_1(u_\epsilon, \chi_\epsilon) \quad \text{and} \quad E_\epsilon(\chi) = \epsilon^n E_1(\chi_\epsilon).$$

Indeed, the total variation scales like ϵ^{n-1}, namely $|D\chi|(\mathbb{R}^n) = \epsilon^{n-1}|D\chi_\epsilon|(\mathbb{R}^n)$. Moreover, $E_{el}(u, \chi) = \epsilon^n E_{el}(u_\epsilon, \chi_\epsilon)$, and therefore $E_{el}(\chi) = \epsilon^n E_{el}(\chi_\epsilon)$, follows by a standard change of variables.

The previous observations justify the following definitions

$$\hat{E}(u, \chi) := E_1(u, \chi) \quad \text{and} \quad \hat{E}(\chi) := E_1(\chi). \tag{11}$$

As a consequence, in what follows we study the scaling behaviour of

$$\hat{E}(V) := \inf\{\hat{E}(\chi) \, : \, |\mathrm{supp}(\chi)| = V\} \tag{12}$$

for different choices of the set K. Undoing the above rescaling, we then obtain the full volume and ϵ-scaling by using the relation

$$\hat{E}(V) = \epsilon^{-n} E_\epsilon(\epsilon^n V). \tag{13}$$

2.3 Small-Volume Regime

A common point for all the following choices of K is the behaviour of the scaled energy $\hat{E}(V)$ when $V \leq 1$.

In this case, the lower bound is a consequence of the isoperimetric inequality, that is

$$\hat{E}(\chi) \gtrsim \mathcal{H}^{n-1}(\partial \, \mathrm{supp}(\chi)) \gtrsim V^{\frac{n-1}{n}}.$$

Remark 2.2 The inequality above holds for every $V > 0$ and provides an *a priori* lower bound for the total energy. In particular, we will use it in the sequel to infer a uniform lower bound for the energy in the large-volume regime. More precisely, if $V > 1$, the above argument always yields that $\hat{E}(\chi) \gtrsim 1$.

For the upper bound we can take e.g. u to be equal to Ax in a ball of radius r, for some $A \in K$, then matching the zero boundary conditions thanks to a cut-off argument on $B_{2r} \setminus B_r$ with $r = V^{\frac{1}{n}}$. Thus, by taking e.g. $\chi = A\chi_{B_{2r}}$,

$$\hat{E}(u, \chi) \lesssim V + V^{\frac{n-1}{n}} \lesssim V^{\frac{n-1}{n}}$$

in this regime of V.

Hence, there exist two constants $C_2 > C_1 > 0$ depending on n and K such that for every $V \leq 1$ we have

$$C_1 V^{\frac{n-1}{n}} \leq \hat{E}(V) \leq C_2 V^{\frac{n-1}{n}}. \tag{14}$$

From (13) we obtain the corresponding scaling law for $E_\epsilon(V)$

$$C_1 \epsilon V^{\frac{n-1}{n}} \leq E_\epsilon(V) \leq C_2 \epsilon V^{\frac{n-1}{n}} \tag{15}$$

for every $V \leq \epsilon^n$.

2.4 Elastic Energy and Fourier Multipliers

In deducing the lower scaling bounds and in order to effectively explore the effects of anisotropy, in this article we will often work in frequency space. Therefore, it is convenient to express the elastic energy in terms of the Fourier transform. To fix notation, for $f \in L^1(\mathbb{R}^n)$, we define

$$\hat{f}(k) := \mathcal{F} f(k) := (2\pi)^{-\frac{n}{2}} \int\limits_{\mathbb{R}^n} e^{-ik \cdot x} f(x) \mathrm{d}x,$$

and use the usual extension argument to also define this for $f \in L^2(\mathbb{R}^n)$. The result below is the analogue of Rüland and Tribuzio (2022, Lemma 4.1) in the case of the full space Fourier transform.

Lemma 2.3 *Let E_{el} be as in (2) and $\chi \in BV(\mathbb{R}^n; K_0)$. Then, there holds*

$$E_{el}(\chi) \geq \sum_{j=1}^{n} \sum_{\ell \neq j} \int_{\mathbb{R}^n} \frac{k_\ell^2}{|k|^2} |\hat{\chi}_{j,j}|^2 \mathrm{d}k. \tag{16}$$

Proof By Plancherel's theorem, the elastic energy can be expressed as

$$E_{el}(u, \chi) = \int_{\mathbb{R}^n} |\hat{u} \otimes ik - \hat{\chi}|^2 \mathrm{d}k. \tag{17}$$

Using that

$$\inf_{u \in H^1(\mathbb{R}^n; \mathbb{R}^n)} \int_{\mathbb{R}^n} |\nabla u - \chi|^2 \mathrm{d}x \geq \inf_{u \in \dot{H}^1(\mathbb{R}^n; \mathbb{R}^n)} \int_{\mathbb{R}^n} |\nabla u - \chi|^2 \mathrm{d}x,$$

we compute the Euler–Lagrange equation associated to the minimization problem

$$\inf_{u \in \dot{H}^1(\mathbb{R}^n; \mathbb{R}^n)} \int_{\mathbb{R}^n} |\nabla u - \chi|^2 \mathrm{d}x$$

on the frequency space, that is

$$(\hat{u} \otimes ik)k = \hat{\chi}k, \quad k \in \mathbb{R}^n.$$

This is solved by $\hat{u}_j = -i \frac{k_j}{|k|^2} \hat{\chi}_{j,j}$ which, inserted in (17), yields the desired result. $\square$

We next introduce some notation. For $0 < \mu < 1$ and $\mu' > 0$, we define

$$C_{j,\mu,\mu'} = \left\{ k \in \mathbb{R}^n : \sum_{\ell \neq j} k_\ell^2 \leq \mu^2 |k|^2, \ |k| \leq \mu' \right\}.$$

Correspondingly, we associate Fourier multipliers $\chi_{j,\mu,\mu'}(D)$ (viewed as operators) to these truncated cones: To this end, we first define $\chi_{j,\mu,\mu'}$ to be positive $C^\infty(\mathbb{R}^n \setminus \{0\})$ functions on the Fourier side such that $\chi_{j,\mu,\mu'}(k) = 1$ for $k \in C_{j,\mu,\mu'}$ and $\chi_{j,\mu,\mu'}(k) = 0$ for $k \in \mathbb{R}^n \setminus C_{j,2\mu,2\mu'}$, satisfying decay conditions as in Marcinkiewicz's multiplier theorem, see for instance Grafakos (2008, Corollary 6.2.5). Given these functions, we then define the Fourier multipliers by their action on $f \in C_c^\infty(\mathbb{R}^n)$ by setting $\chi_{j,\mu,\mu'}(D)f := \mathcal{F}^{-1}(\chi_{j,\mu,\mu'} \mathcal{F} f)$, where $\chi_{j,\mu,\mu'} \mathcal{F} f$ denotes the usual multiplication of functions.

2.5 Estimates in the Frequency Space

The following two results are the corresponding versions of those in Rüland and Tribuzio (2021, Sect. 4) adapted to the case of the continuous Fourier transform (rather than Fourier series). They encode a first frequency localization using elastic and surface energies (Lemma 2.4) and an iteration of this through a commutator argument (Lemma 2.5). The proofs can be obtained by the ones from Rüland and Tribuzio (2021) by just replacing sums with integrals. We therefore omit the repetition of these proofs.

Lemma 2.4 (Lemma 4.5, Rüland and Tribuzio 2021) *Let $n \geq 2$ and K be fixed. Let $\chi \in BV(\mathbb{R}^n; K_0)$, let $E_{el}(\chi)$ be as in (2) and $E_{surf}(\chi) := |D\chi|(\mathbb{R}^n)$. Then there exists a constant $C > 0$ depending on n and K such that for every $0 < \mu < 1$, $\mu_2 > 0$ there holds*

$$\sum_{j=1}^n \|\chi_{j,j} - \chi_{j,\mu,\mu_2}(D)\chi_{j,j}\|_{L^2}^2 \leq C(\mu^{-2} E_{el}(\chi) + \mu_2^{-1} E_{surf}(\chi)).$$

Lemma 2.5 (Corollary 4.9, Rüland and Tribuzio 2021) *Let K, n and χ be as in the statement of Lemma 2.4. Let $\ell \in \{1, \ldots, n\}$ and let g be a polynomial such that for some $\lambda_j \in \mathbb{R}$, $j \in \{1, \ldots, n\}$ there holds*

$$\chi_{\ell,\ell} = g\left(\sum_{j \neq \ell} \lambda_j \chi_{j,j} \right).$$

Let $0 < \mu < 1$, $\mu', \mu'' > 0$ and $\tilde{\mu} = M\mu\mu''$ for some constant $M > 1$ depending on the degree of g. Then for every $\gamma \in (0, 1)$ there exists a constant $C > 0$ depending on

n, g, K and γ such that there holds

$$\|\chi_{\ell,\ell} - \chi_{\ell,\mu,\tilde{\mu}}(D)\chi_{\ell,\ell}\|_{L^2}^2 \leq C \sum_{j \neq \ell} |\lambda_j| \psi_\gamma \left(\|\chi_{j,j} - \chi_{j,\mu,\mu''}(D)\chi_{j,j}\|_{L^2}^2 \right)$$
$$+ C \|\chi_{\ell,\ell} - \chi_{\ell,\mu,\mu'}(D)\chi_{\ell,\ell}\|_{L^2}^2,$$

where $\psi_\gamma(z) = \max\{z, z^{1-\gamma}\}$.

Let us comment on Lemma 2.5: We view this as a "commutator" bound, in that we roughly commute the Fourier multiplier $\frac{k_\ell^2}{|k|^2}$ from the energy (16) and the polynomial g from Lemma 2.5. It is this nonlinear relation which is crucially exploited in our arguments below and allows us to bootstrap the energy estimates in a quantitative way. In what follows we will apply Lemma 2.5 for the derivation of lower bounds for higher-order laminates. Here we will always apply the result with $0 < \tilde{\mu} \leq \mu'' \leq \mu' < 1$ in order to improve on the possible region of Fourier space concentration.

We conclude this section by giving the following control of low frequencies.

Lemma 2.6 *Let $\varphi \in L^2(\mathbb{R}^n) \cap L^1(\mathbb{R}^n)$, $0 < \mu < 1$, $\mu' > 0$ and let $j \in \{1, \ldots, n\}$. Then, there exists a constant $C > 0$ depending on n such that*

$$\int_{C_{j,\mu,\mu'}} |\hat{\varphi}|^2 \mathrm{d}k \leq C \|\varphi\|_{L^1}^2 (\mu')^n \mu^{n-1}.$$

Proof The argument follows from the L^1-L^∞ bound for the Fourier transform. Indeed,

$$\int_{C_{j,\mu,\mu'}} |\hat{\varphi}|^2 \mathrm{d}k \leq \left(\sup_{k \in \mathbb{R}^n} |\hat{\varphi}| \right)^2 |C_{j,\mu,\mu'}| \leq C \|\varphi\|_{L^1}^2 (\mu')^n \mu^{n-1}.$$

<div align="right">□</div>

3 First-Order Laminates: The 1+1-Well Case

We start our discussion of the outlined nucleation results by considering the simplest situation possible, i.e. $\#K = 1$. A more general version of this problem has been studied in Knüpfer and Kohn (2011), in the context of geometrically linearized elasticity.

We translate the results from Knüpfer and Kohn (2011) into our context.

Theorem 5 (Theorem 2.1, Knüpfer and Kohn 2011) *Let $K = \{A\}$ for some $A \in diag(n, \mathbb{R})$ with $\mathrm{rank}(A) = 1$ and let $\hat{E}(V)$ be as in (12). Then there exist two positive constants $C_2 > C_1 > 0$ depending on K and n such that for every $V > 0$ there holds*

$$C_1 \hat{r}(V) \leq \hat{E}(V) \leq C_2 \hat{r}(V), \quad where \quad \hat{r}(V) = \begin{cases} V^{\frac{n-1}{n}} & V \leq 1, \\ V^{\frac{2n-2}{2n-1}} & V \geq 1. \end{cases}$$

Proof As in Knüpfer and Kohn (2011) the proof of this result consists of two parts: An upper bound and a lower bound. The upper bound construction from Knüpfer and Kohn (2011) does not make use of gauge invariance but only the presence of a rank-one connection between the two phases. As a consequence, it also works in our context with essentially no modification.

The proof of the lower bound in Knüpfer and Kohn (2011) consists of two steps: The derivation of a localized lower bound estimate (Knüpfer and Kohn 2011 (Proposition 3.1)) stating that if little of the minority phase and only small perimeter is present, then a good lower bound estimate holds true. Translated to our context, it reads:

Claim 3.1 *Let $R > 0$ and let $\chi \in BV(\mathbb{R}^n; K_0)$. Then there exist universal constants $c_n, \alpha > 0$ (depending only on the dimension $n \in \mathbb{N}$) such that if*

$$\|\chi\|_{L^1(B_R)} \leq c_n R^n \quad and \quad |D\chi|(B_R) \leq c_n R^{n-1}, \tag{18}$$

then

$$\inf_{u \in H^1(\mathbb{R}^n;\mathbb{R}^n)} \int_{B_R} |\nabla u - \chi|^2 \mathrm{d}x \geq c_n R^{-n} \|\chi\|^2_{L^1(B_{\alpha R})}.$$

Exploiting this, the full lower bound is proved by a covering argument. Since there is no difference in the covering argument, we only discuss Knüpfer and Kohn (2011, Proposition 3.1) which in turn relies on Knüpfer and Kohn (2011, Lemma 3.2), its two-dimensional analogue. For convenience of the reader and for completeness, we retrace the main ideas of the proof of Knüpfer and Kohn (2011, Lemma 3.2), being more specific in the parts that differ in our context.

Ideas of the proof of Claim 3.1 *for $n = 2$:* Without loss of generality we consider $A = e_1 \otimes e_1$ and $R = 1$. Further, as in Knüpfer and Kohn (2011) we fix $\alpha = \frac{1}{5}$. Following Knüpfer and Kohn (2011), we now argue by contradiction, that is letting $\mu := \|\chi\|_{L^1(B_\alpha)}$ we assume that for every $c_2 > 0$ such that (18) holds there exists $u \in H^1(\mathbb{R}^2; \mathbb{R}^2)$ such that

$$\|\partial_1 u_1 - \chi_{1,1}\|_{L^2(B_1)} + \|\partial_2 u_2\|_{L^2(B_1)} + \|\partial_2 u_1\|_{L^2(B_1)} + \|\partial_1 u_2\|_{L^2(B_1)} \leq c_2\mu. \tag{19}$$

We split the argument leading to the contraction into several steps.

Steps 1 and 2: We consider three rectangles $Q^{(i)} = \left[l_1^{(i)}, l_2^{(i)}\right] \times [-h, h]$ with $l_1^{(i)} < l_2^{(i)}, l_2^{(i)} = l_1^{(i+1)}$ such that $l_2^{(3)} - l_1^{(1)}, 2h \leq 1$ and

$$Q^{(2)} \supset B_\alpha, \quad Q^{(i)} \subset B_{3\alpha}, \ i \in \{1, 2, 3\}.$$

We also denote $I_1^{(i)} = [l_1^{(i)}, l_2^{(i)}], i \in \{1, 2, 3\}, I_1 = [l_1^{(1)}, l_2^{(3)}]$ and $I_2 = [-h, h]$. Up to small translations of $Q^{(i)}$ exploiting (18) and the fact that c_2 can be chosen to be arbitrarily small one proves $\|\chi\|_{L^1(\partial Q^{(i)})}, |D\chi|(\partial Q^{(i)}) = 0$. This, combined with (19), implies also that

$$\int_{\partial Q^{(i)}} |\nabla u|^2 = \int_{\partial Q^{(i)}} |\nabla u - \chi|^2 \leq c_2\mu. \tag{20}$$

Moreover, by possibly passing from u_1 to $u_1 - \langle u_1 \rangle_{I_1 \times \{h\}}$ we may assume that $\langle u_1 \rangle_{I_1 \times \{h\}} = 0$. Here and in the rest of the proof, with a slight abuse of notation, we write $\langle u_1 \rangle_{I \times \{y\}} = \frac{1}{|I|} \int_I u_1(t, y) \mathrm{d}t$ and $\langle u_1 \rangle_{I \times J} = \frac{1}{|I||J|} \int_{I \times J} u_1(t, s) \mathrm{d}t \mathrm{d}s$ for every interval $I, J \subset \mathbb{R}$ and $y \in \mathbb{R}$.

Steps 3 and 4: We show that u_1 is close to zero in mean inside $Q^{(i)}$ for $i \in \{1, 2, 3\}$. We begin by proving that u_1 is close to 0 on the horizontal boundaries of $Q^{(i)}$. Indeed for every $x \in I_1^{(i)}$, by the fundamental theorem of calculus, Hölder's inequality and (20)

$$|u_1(x, \pm h) - \langle u_1 \rangle_{I_1^{(i)} \times \{\pm h\}}| \leq \|\partial_1 u_1\|_{L^2(I_1^{(i)} \times \{\pm h\})} \leq c_2 \mu. \tag{21}$$

Moreover,

$$|\langle u_1 \rangle_{I_1^{(i)} \times \{h\}} - \langle u_1 \rangle_{I_1^{(i)} \times \{-h\}}| \leq \int_{I_1^{(i)}} \int_{-h}^{h} |\partial_2 u_1(x, t)| \mathrm{d}t \mathrm{d}x \leq \|\partial_2 u_1\|_{L^2(I_1^{(i)} \times I_2)} \leq c_2 \mu.$$

Due to our normalization $\langle u_1 \rangle_{I_1 \times \{h\}} = 0$ and (21), we thus obtain that

$$\|u_1\|_{L^\infty(I_1^{(i)} \times \{\pm h\})} \leq 2 c_2 \mu.$$

Combined with the off-diagonal bounds in (19) this yields

$$|\langle u_1 \rangle_{Q^{(i)}}| \leq 3 c_2 \mu, \quad i \in \{1, 2, 3\}. \tag{22}$$

Step 5: Finally, let $x_1^* \in I_1^{(1)}$ be such that $\langle u_1 \rangle_{Q^{(1)}} = \frac{1}{|I_2|} \int_{I_2} u_1(x_1^*, t) \mathrm{d}t$. Then, using that $u_1(x_1, x_2) = u_1(x_1^*, x_2) + \int_{x_1^*}^{x_1} \partial_1 u_1(t, x_2) \mathrm{d}t$, we have

$$\langle u_1 \rangle_{Q^{(3)}} = \langle u_1 \rangle_{Q^{(1)}} + \left\langle \int_{x_1^*}^{\cdot} \partial_1 u_1(t, \cdot) \mathrm{d}t \right\rangle_{Q_3}$$

$$\geq \langle u_1 \rangle_{Q^{(1)}} + \frac{1}{|I_2|} \mu + \left\langle \int_{x_1^*}^{\cdot} \partial_1 u_1(t, \cdot) - \chi(t, \cdot) \mathrm{d}t \right\rangle_{Q^{(3)}},$$

where in the last step we have used that $I_1^{(2)} \subset (x_1^*, x_1)$ for every $x_1 \in I_1^{(3)}$ and that $Q^{(2)} \supset B_\alpha$. The inequality above yields from (19) by taking c_2 small enough, that

$$\langle u_1 \rangle_{Q^{(3)}} - \langle u_1 \rangle_{Q^{(1)}} \geq \left(\frac{1}{|I_2|} - c_2 \right) \mu.$$

This contradicts (22) by further reducing c_2 if needed, and the claim is proved. □

The remainder of the argument for Theorem 1 then follows as in Knüpfer and Kohn (2011). □

4 First-Order Laminates: The 2+1-Wells Case

In this section, we discuss the proof of Theorem 2, i.e. the setting in which

$$K = \{A, B\}, \quad \text{with} \quad A = \begin{pmatrix} -\lambda & 0 \\ 0 & 0 \end{pmatrix}, \ B = \begin{pmatrix} 1-\lambda & 0 \\ 0 & 0 \end{pmatrix} \tag{23}$$

for some $\lambda \in (0, 1)$ fixed, with "austenite" given by the zero matrix.

In this setting, after the normalization outlined above, we seek to prove the following bounds:

Theorem 6 *Let $\hat{E}(V)$ be as in (12) and let K be as in (23). Then there exist two positive constants $C_2 > C_1 > 0$ depending on K such that for every $V > 0$ there holds*

$$C_1 \hat{r}(V) \leq \hat{E}(V) \leq C_2 \hat{r}(V), \quad \text{where} \quad \hat{r}(V) = \begin{cases} V^{\frac{1}{2}} & \text{if } V \leq 1, \\ V^{\frac{3}{5}} & \text{if } V > 1. \end{cases}$$

Rescaling this as in (13) then implies the claim of Theorem 2.

In order to infer these bounds, we argue in two steps: First, in Proposition 4.1 we deduce lower bounds. Next, in Proposition 4.2, we provide an upper bound construction. Combining these observations with the small volume estimates from Sect. 2.3 and the normalization arguments from Sect. 2.2 then implies the claim from Theorems 2 and 6.

4.1 Lower Bounds

In deducing the lower bounds, we first seek to prove the following proposition:

Proposition 4.1 *Let $\hat{E}(V)$ be as in (12) and let K be as in (23). Then for every $V > 1$ there holds*

$$\hat{E}(V) \gtrsim V^{3/5}. \tag{24}$$

Proof Let $0 < \mu < 1, \mu_2 > 0$ be two constants which are to be determined below. We estimate as follows by means of Lemmas 2.4 and 2.6:

$$\begin{aligned}
\min\{\lambda^2, (1-\lambda)^2\}V \leq \|\chi_{1,1}\|_{L^2}^2 &\leq \|\chi_{1,\mu,\mu_2}(D)\chi_{1,1}\|_{L^2}^2 + \|\chi_{1,1} - \chi_{1,\mu,\mu_2}(D)\chi_{1,1}\|_{L^2}^2 \\
&\leq C \max\{\lambda^2, (1-\lambda)^2\}\mu_2^2 \mu V^2 + C\mu^{-2} E_{el}(\chi) + C\mu_2^{-1} E_{surf}(\chi) \\
&\leq C \max\{\lambda^2, (1-\lambda)^2\}\mu_2^2 \mu V^2 + C(\mu^{-2} + \mu_2^{-1})\hat{E}(\chi).
\end{aligned}$$

With the choice $\mu = \frac{1}{2C} \min\left\{\frac{\lambda^2}{(1-\lambda)^2}, \frac{(1-\lambda)^2}{\lambda^2}\right\} \frac{1}{\mu_2^2 V}$ we obtain

$$\min\{\lambda^2, (1-\lambda)^2\}V \leq C'(\mu_2^4 V^2 + \mu_2^{-1})\hat{E}(\chi),$$

for some $C' > 0$. We further optimize the right hand side in μ_2 which yields $\mu_2 \sim V^{-\frac{2}{5}}$. Inserting this into the estimate and rearranging then yields the claim. $\qquad\square$

4.2 Upper Bounds

We now deal with an upper bound construction. For this we present two types of constructions: One directly using branchings in thin long domains aligned with the direction of lamination, the other exploiting the flexibility of the domain more effectively by working in diamond- or lens-shaped domains. Since the latter are also observed in experiments (Niemann et al. 2017; Schwabe et al. 2021; Tan and Huibin 1990), we present the diamond-shaped constructions (see Fig. 3) in the main body of the text and postpone the rectangular ones to the appendix. Diamond-shaped constructions which in addition incorporate additional determinant constraints have been used in Conti (2008).

Proposition 4.2 *Let $\hat{E}(u, \chi)$ be as in (11), let K be as in (23) and let $V > 1$ be given. Then there exist a compact, connected set $\Omega \subset \mathbb{R}^2$ with Lipschitz boundary, $|\Omega| = V$, $u \in W_0^{1,\infty}(\Omega; \mathbb{R}^2)$ and $\chi \in BV(\mathbb{R}^2; K_0)$ with $\mathrm{supp}(\chi) = \Omega$ such that*

$$\hat{E}(u, \chi) \lesssim V^{\frac{3}{5}}.$$

Proof Given $H > L > 1$, we take the rhombus

$$\Omega = \mathrm{conv}\left(\left\{(0, 0), \left(\lambda L, \frac{H}{2}\right), \left(\lambda L, -\frac{H}{2}\right), (L, 0)\right\}\right).$$

Consider $u : \mathbb{R}^2 \to \mathbb{R}^2$ with $u_2 \equiv 0$ and u_1 defined by integration in order to attain zero boundary condition on $\partial\Omega$ and having $\partial_1 u_1 = 1 - \lambda$ in $\Omega \cap ((0, \lambda L) \times \mathbb{R})$ and $\partial_1 u_1 = -\lambda$ in $\Omega \cap ((\lambda L, L) \times \mathbb{R})$, that is

$$u_1(x_1, x_2) = \begin{cases} (1 - \lambda)\left(x_1 - \dfrac{2\lambda L}{H}|x_2|\right) & \dfrac{2\lambda L}{H}|x_2| \leq x_1 \leq \lambda L, \\ \lambda\left(-x_1 - \dfrac{2(1 - \lambda)L}{H}|x_2| + L\right) & \lambda L \leq x_1 \leq L - \dfrac{2(1-\lambda)L}{H}|x_2|, \\ 0 & \text{otherwise.} \end{cases}$$

In particular, $u \in W_0^{1,\infty}(\Omega; \mathbb{R}^2)$. Let $\chi \in BV(\mathbb{R}^2; K_0)$ be the projection of ∇u onto K_0. Noticing that $\partial_1 u_1 \equiv \chi_{1,1}$, we obtain

$$E_{el}(u, \chi) = \int_\Omega |\partial_2 u_1|^2 \mathrm{d}x \leq \frac{L^3}{2H} \quad \text{and} \quad E_{\text{surf}}(\chi) \leq H + 2\sqrt{\frac{H^2}{4} + L^2}.$$

Hence,

$$\hat{E}(u, \chi) \lesssim \frac{L^3}{H} + H,$$

Fig. 3 The graph of (the non-trivial component of) a two-dimensional inclusion which attains the upper bound. Different colors represent different phases, black lines are the jump set of the phase-indicator function; on dashed lines the gradient jumps inside the same phase
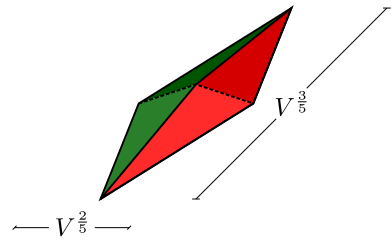
and by an optimization argument we obtain $L \sim H^{\frac{2}{3}}$ which implies $V \sim H^{\frac{5}{3}}$, and the result follows.   □

Remark 4.3 Note that the lower bound of Proposition 4.1 is ansatz-free and therefore does not give any information on optimal structures for u and χ. On the other side, the upper bound of Proposition 4.2 provides some information in that direction. In particular, we know that we can achieve the optimal energy scaling with structures supported in "thin" domains of height $V^{\frac{3}{5}}$ and width $V^{\frac{2}{5}}$. We however expect that the analysis of the optimal shape requires a more detailed study of the Euler–Lagrange equations associated with our energies.

4.3 Proof of Corollary 1.1

Finally, we provide the proof of Corollary 1.1 which allows us to generalize the previous scaling law to arbitrary dimensions.

Proof of Corollary 1.1 We split the proof into two steps:

Step 1: Lower bounds. The results in the small volume regimes directly follow from the isoperimetric considerations from Sect. 2.3. In the case $V > 1$ (in the normalized setting), retracing the proof of Proposition 4.1 in dimension n, we derive

$$V \lesssim \mu^{n-1}\mu_2^n V^2 + (\mu^{-2} + \mu_2^{-1})\hat{E}(\chi)$$

yielding, after optimization, the choices $\mu \sim V^{-\frac{1}{3n-1}}$, $\mu_2 \sim V^{-\frac{2}{3n-1}}$ and the lower bound

$$V^{\frac{3n-3}{3n-1}} \lesssim \hat{E}(\chi).$$

Step 2: Upper bounds. Again we first provide a lens-shaped construction for the upper bound analogously as done in the two-dimensional case in the proof of Proposition 4.2. A second argument in a thin rectangle is included in the appendix. Our n-dimensional construction consists of a diamond-shaped inclusion whose lamination direction is "very thin" with respect to the others. For the sake of simplicity, we first consider the special case $K = \{\pm e_1 \otimes e_1\} \subset \mathbb{R}^{n \times n}$ from which we recover the case from the corollary by carrying out a change of variables at the end of the proof.

For $H > L > 1$ consider the domain

$$\Omega = \mathrm{conv}\left(\left\{\pm \frac{L}{2}e_1, \left\{\pm \frac{H}{2}e_j\right\}_{j=2}^n\right\}\right).$$

We consider $u : \mathbb{R}^n \to \mathbb{R}^n$ with $u_j \equiv 0$ for $j \in \{2, \ldots, n\}$ and

$$u_1(x) = \begin{cases} |x_1| + \frac{L}{H}(|x_2| + \cdots + |x_n|) - \frac{L}{2} & x \in \Omega, \\ 0 & \text{otherwise.} \end{cases}$$

Notice that $u \in W_0^{1,\infty}(\Omega; \mathbb{R}^n)$ with $\|\nabla u\|_{L^\infty} \lesssim 1$. Let χ denote the projection of ∇u onto K_0. Then we have $\chi = e_1 \otimes e_1$ on $\Omega \cap ((0, +\infty) \times \mathbb{R}^{n-1})$ and $\chi = -e_1 \otimes e_1$ on $\Omega \cap ((-\infty, 0) \times \mathbb{R}^{n-1})$. Hence,

$$E_{el}(u, \chi) \lesssim |\Omega|\frac{L^2}{H^2} \lesssim L^3 H^{n-3} \quad \text{and} \quad E_{\mathrm{surf}}(\chi) \lesssim H^{n-1}.$$

This implies that $\hat{E}(u, \chi) \lesssim L^3 H^{n-3} + H^{n-1}$. Optimizing this we get $L \sim H^{\frac{2}{3}}$ which yields the desired result from the volume constraint.

Now we return to the general case. Given K be as in the statement, we consider the Lipschitz map $\phi(x_1, x_2, \ldots, x_n) = (\phi_1(x_1), x_2, \ldots, x_n)$ with

$$\phi_1(t) = \begin{cases} \lambda t & t < 0 \\ (1 - \lambda)t & t \geq 0 \end{cases},$$

and define $\tilde{u}(x) := u(\phi(x))$ and $\tilde{\chi}(x) := \chi(\phi(x))\nabla\phi(x)$, where u and χ are the functions defined in the first part of the proof above. Then, $\tilde{\chi} \in K_0$, the inclusion domain is

$$\tilde{\Omega} = \mathrm{supp}(\tilde{\chi}) = \mathrm{conv}\left(\left\{-\frac{L}{2\lambda}e_1, \frac{L}{2(1-\lambda)}e_1, \left\{\pm \frac{H}{2}e_j\right\}_{j=2}^n\right\}\right),$$

$\tilde{u} \in W_0^{1,\infty}(\tilde{\Omega}; \mathbb{R}^n)$ and there holds

$$\hat{E}(\tilde{u}, \tilde{\chi}) \leq \max\{\lambda^{-1}, (1-\lambda)^{-1}\}\hat{E}(u, \chi).$$

Hence the result follows. $\square$

Remark 4.4 Theorem 2 and Corollary 1.1 can be stated in a slightly more general way, that is replacing K with $\tilde{K} = \{A, B\} \subset \mathbb{R}^{n \times n}$ such that $\mathrm{rank}(A - B) = 1$, and $0 = \lambda A + (1 - \lambda)B$ for some $\lambda \in (0, 1)$. The only matrices complying with such linear constraints have the following structure: $A = (1 - \lambda)a \otimes v$, $B = -\lambda a \otimes v$ with $a, v \in \mathbb{R}^n \setminus \{0\}$ and $|v| = 1$. Then, the same scaling results can be obtained by a simple change of variable.

Indeed, let $R_a, R_v \in SO(n)$ be the rotations such that $R_a a = |a|e_1$ and $R_v v = e_1$. For every $\chi \in BV(\mathbb{R}^2; \tilde{K} \cup \{\mathbf{0}\})$ and $u \in H^1(\mathbb{R}^2; \mathbb{R}^2)$ we define $\tilde{u}(x) := \frac{1}{|a|} R_a u(R_v^{-1} x)$ and $\tilde{\chi}(x) := \frac{1}{|a|} R_a \chi(R_v^{-1} x) R_v^{-1}$. Hence, by the fact that $R_a(a \otimes v) R_v^{-1} = |a|e_1 \otimes e_1$, $\tilde{\chi} \in BV(\mathbb{R}^2; K_0)$, $u \in H^1(\mathbb{R}^2; \mathbb{R}^2)$, and the following two equalities hold

$$E_{el}(u, \chi) = \frac{1}{|a|^2} E_{el}(\tilde{u}, \tilde{\chi}), \quad E_{\text{surf}}(\chi) = \frac{1}{|a|} E_{\text{surf}}(\tilde{\chi}).$$

Eventually, denoting with $\tilde{E}_\epsilon$ the minimum problem in (4) corresponding to $\tilde{K}$ we conclude that

$$\tilde{C}_1 E_\epsilon(V) \leq \tilde{E}_\epsilon(V) \leq \tilde{C}_2 E_\epsilon(V),$$

with $\tilde{C}_2 \geq \tilde{C}_1 > 0$ being constants depending on $\tilde{K}$.

5 A Second-Order Laminate: An Example of a 4+1-Wells Case

We next proceed to the analysis of second-order laminates. In this section, it is our main objective to prove the claim of Theorem 3. We recall that in this setting, in particular, the zero matrix belongs to K^{lc} and can be obtained as

$$\frac{1}{2}\left(\frac{1}{3}A_1 + \frac{2}{3}A_2\right) + \frac{1}{2}\left(\frac{1}{3}A_3 + \frac{2}{3}A_4\right) = \mathbf{0},$$

that is the zero matrix is a second-order laminate of K. A convenient way to write the elastic energy is the following

$$E_{el}(u, \chi) = \int_{\mathbb{R}^2} \left|\nabla u - \chi_1 A_1 - \chi_2 A_2 - \chi_3 A_3 - \chi_4 A_4\right|^2 dx$$

with $\chi_j \in BV(\mathbb{R}^2; \{0, 1\})$ and $\chi_1 + \chi_2 + \chi_3 + \chi_4 \leq 1$. In terms of the phase indicator χ, we have $\chi = \sum_{j=1}^4 \chi_j A_j$, hence $\chi_{1,1} = -\chi_1 - \chi_2 + \chi_3 + \chi_4$ and $\chi_{2,2} = -2\chi_1 + \chi_2 + 2\chi_3 - \chi_4$.

With this notation we can write the first diagonal component in terms of the second diagonal component as follows

$$\chi_{1,1} = g(\chi_{2,2}), \tag{25}$$

where g is a polynomial of degree 3. The choice of g is not unique and it can be made explicit e.g. by interpolation. An example of such a polynomial is $g(t) = \frac{1}{2}t^3 - \frac{3}{2}t$. Notice that the condition $g(0) = 0$ ensures that (25) is globally satisfied, in particular also outside the inclusion domain. As before, by rescaling and the small volume energy bounds from Sect. 2, it suffices to prove the following result:

Theorem 7 *Let $\hat{E}(V)$ be as in* (12) *and let K be as in* (6). *Then, there exist two positive constants $C_2 > C_1 > 0$ depending on K such that for every $V > 0$ there holds*

$$C_1 \hat{r}(V) \leq \hat{E}(V) \leq C_2 \hat{r}(V), \quad where \quad \hat{r}(V) = \begin{cases} V^{\frac{1}{2}} & if \ V \leq 1, \\ V^{\frac{5}{7}} & if \ V > 1. \end{cases}$$

As above, we split this into two steps: In Proposition 5.1 we first deduce corresponding lower bounds and in Proposition 5.2 we provide matching upper bounds. Using the considerations from Sects. 2.2 and 2.3 then implies the desired claim of Theorem 7.

5.1 Lower Bounds

We first give a lower bound for the large inclusion regime.

Proposition 5.1 *Let $\hat{E}(V)$ be as in* (12), *and let K be as in* (6). *Then for every $V > 1$ there holds*

$$\hat{E}(V) \gtrsim V^{\frac{5}{7}}. \tag{26}$$

Proof Let $0 < \mu, \mu_2 < 1$ be constants to be determined and let $\mu_3 = M\mu\mu_2$ for some $M > 1$ depending on g. We begin by observing that

$$V = \|\chi_{1,1}\|_{L^2}^2 \leq 2\|\chi_{1,\mu,\mu_3}(D)\chi_{1,1}\|_{L^2}^2 + 2\|\chi_{1,1} - \chi_{1,\mu,\mu_3}(D)\chi_{1,1}\|_{L^2}^2. \tag{27}$$

By virtue of Lemma 2.6, we control the first term on the right-hand side of (27) by

$$\|\chi_{1,\mu,\mu_3}(D)\chi_{1,1}\|_{L^2}^2 \leq C\mu\mu_3^2 V^2. \tag{28}$$

Applying Lemma 2.5 with $\mu' = \mu'' = \mu_2$ thanks to relation (25) we also get

$$\begin{aligned}\|\chi_{1,1} - \chi_{1,\mu,\mu_3}(D)\chi_{1,1}\|_{L^2}^2 &\leq C\|\chi_{1,1} - \chi_{1,\mu,\mu_2}(D)\chi_{1,1}\|_{L^2}^2 \\ &\quad + C_\gamma \psi_\gamma \left(\|\chi_{2,2} - \chi_{2,\mu,\mu_2}(D)\chi_{2,2}\|_{L^2}^2\right),\end{aligned}$$

which, by Lemma 2.4 and the facts that $z \leq \psi_\gamma(z)$ and $\psi_\gamma(\delta z) \leq \delta\psi_\gamma(z)$ for every $z > 0$ and $\delta > 1$, can be further reduced to

$$\|\chi_{1,1} - \chi_{1,\mu,\mu_3}(D)\chi_{1,1}\|_{L^2}^2 \leq C_\gamma (\mu^{-2} + \mu_2^{-1})\psi_\gamma\left(\hat{E}(\chi)\right). \tag{29}$$

Gathering (27)–(29) we then arrive at

$$V \leq C\mu\mu_3^2 V^2 + C_\gamma(\mu^{-2} + \mu_2^{-1})\psi_\gamma\left(\hat{E}(\chi)\right).$$

Now, recalling that $\mu_3 \sim \mu \mu_2$, we choose μ_2 such that $\mu^3 \mu_2^2 V^2 \sim V$, that is $\mu_2 \sim V^{-\frac{1}{2}} \mu^{-\frac{3}{2}}$. Such a choice yields

$$V \le C_\gamma (\mu^{-2} + V^{\frac{1}{2}} \mu^{\frac{3}{2}}) \psi_\gamma (\hat{E}(\chi)),$$

where we have possibly increased the constant C_γ. Optimizing we choose $\mu \sim V^{-\frac{1}{7}}$ and therefore obtain that

$$V \le C_\gamma V^{\frac{2}{7}} \psi_\gamma (\hat{E}(\chi)),$$

which implies

$$V^{\frac{5}{7}} \lesssim \psi_\gamma (\hat{E}(\chi)). \tag{30}$$

From the condition $V > 1$ and Remark 2.2 we have $\hat{E}(\chi) \gtrsim 1$. As a consequence, $\psi_\gamma (\hat{E}(\chi)) \lesssim \hat{E}(\chi)$, and (30) implies the desired lower bound.   □

5.2 Upper Bounds

We next turn to an upper bound construction in the large volume regime for which we show a matching upper bound.

Proposition 5.2 *Let $\hat{E}(u, \chi)$ be as in (11), let K be as in (6) and let $V > 1$ be given. Then there exist $\Omega \subset \mathbb{R}^2$ compact, connected, with Lipschitz boundary and $|\Omega| = V$, $u \in W_0^{1,\infty}(\Omega; \mathbb{R}^2)$ and $\chi \in BV(\mathbb{R}^2; K_0)$ with $\mathrm{supp}(\chi) = \Omega$ such that*

$$\hat{E}(u, \chi) \lesssim V^{\frac{5}{7}}.$$

As above, we again present two possible proofs of this result: A construction in a thin rectangle with double branching (given in Section A.3 in the Appendix) and a construction in a thin diamond/lens with simple branching. The latter exploits the more flexible domain geometry by consisting of a lens/diamond shape. We highlight that the self-similar argument exploited for building the geometry of the construction below takes its inspiration from those used in Kohn and Wirth (2016), Knüpfer et al. (2013).

Proof of Proposition 5.2 by means of a construction with a lens-type shape. For $H > 2L > 1$ we consider the rhombus

$$\Omega = \mathrm{conv}\left(\left\{\left(-\frac{L}{2}, 0\right), \left(0, \frac{H}{2}\right), \left(0, -\frac{H}{2}\right), \left(0, \frac{L}{2}\right)\right\}\right).$$

As a first step we consider the construction given in Proposition 4.2 with gradients

$$B_1 = \frac{1}{3} A_1 + \frac{2}{3} A_2 \quad \text{and} \quad B_2 = \frac{1}{3} A_3 + \frac{2}{3} A_4.$$

This corresponds to the macroscopic deformation. This macroscopic deformation will be replaced by a microscopic deformation which is achieved by a construction of fine scale oscillations between phases A_1 and A_2 on the left part of the domain and between A_3 and A_4 on the right part. We work in several steps.

Step 1: Definition of a macroscopic state. We consider w to be obtained analogously as in the proof of Proposition 4.2 with K replaced by the set $\{B_1, B_2\}$, that is $w = (w_1, 0)$ with

$$w_1(x_1, x_2) = \begin{cases} -\frac{L}{2} + |x_1| + \frac{L}{H}|x_2| & x \in \Omega, \\ 0 & \text{otherwise.} \end{cases}$$

The function w will play the role of a macroscopic state. We highlight that the construction from Proposition 4.2 does not give deformations exactly equal to B_1, B_2 but involves slight perturbations of these (which are of the form $\pm \frac{L}{H} e_1 \otimes e_2$, see the discussion in Step 4 below).

Step 2: Branching building block. We now define a single tree of a branching construction on a general rectangle $R := [0, \ell] \times [0, h]$ with $\ell > 4h$. By applying Rüland and Tribuzio (2021, Lemma 3.2) with inverted roles of x_1 and x_2 and with $N = 1$, we obtain $v^{j,R} \in W^{1,\infty}(R; \mathbb{R}^2)$ such that $v^{j,R} = B_j x$ on ∂R and

$$\hat{E}(v^{j,R}, \chi^{j,R}) \lesssim \frac{h^3}{\ell} + \ell, \tag{31}$$

where $\chi^{j,R}$ is the projection of $\nabla v^{j,R}$ onto the set $\{A_1, A_2\}$ or $\{A_3, A_4\}$ if $j = 1$ or 2 respectively. Note that, by translation invariance, the same construction (still matching $B_j x$ at the boundary) can be obtained in rectangles $x + R$ for any $x \in \mathbb{R}^2$.

Step 3: Subdivision of the domains into rectangles. We subdivide the domain Ω into rectangles having the same ratio between width and height. The correct ratio will be then obtained in Step 5 via optimization. We work in the triangular subdomain $T = \text{conv}\big(\{(-\frac{L}{2}, 0), (0, \frac{H}{2}), (0, 0)\}\big)$ recovering the full subdivision symmetrically.

We fix $0 < r < \frac{H}{2}$ a parameter to be determined later. We cut T into horizontal slices at height h_j, with $h_0 = 0$, $h_1 = r$ and $h_{j+1} > h_j$. In each of these slices we consider the maximal rectangle contained in T, that is

$$R_j := [-\ell_j, 0] \times [h_j, h_j + r_j],$$
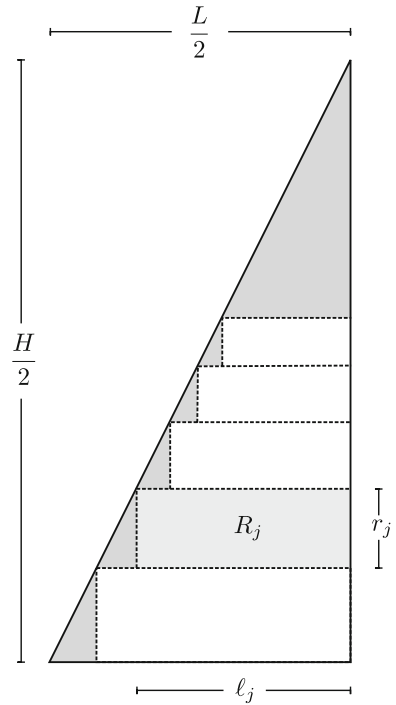$$\text{with } r_j := h_{j+1} - h_j, \quad \ell_j := \sup\{\ell : (-\ell, h_{j+1}) \in T\}. \tag{32}$$

We choose r_j so that the rectangles R_j have the same ratio between width and height. Solving recursively $r_j = \frac{r}{\ell_0} \ell_j$, we find

$$r_j = r\left(1 - \frac{2}{H}r\right)^j \quad \text{and} \quad \ell_j = \frac{L}{2}\left(1 - \frac{2}{H}r\right)^{j+1}.$$

We make this subdivision for $0 \leq j \leq j_0$, with j_0 being the largest index such that $h_{j_0} < \frac{H-L}{2}$. In the end, we also define $T_0 = \bigcup_{j=0}^{j_0} R_j$ (see Fig. 4).

Fig. 4 Subdivision of T into rectangles R_j. The shaded region is $T \setminus T_0$

Step 4: Definition of u. We define u to be a fine-scale branching oscillation inside R_j and being equal to the macroscopic state w on $T \setminus T_0$. To do so, we slightly modify the functions obtained in Step 2 with an affine perturbation in order to match the macroscopic state w at ∂R_j (which is close to an affine function with gradient B_1 or B_2 but is not exactly equal to one these, see the comment in Step 1 above). Thus, for every $x \in T$ we define

$$u(x) = \begin{cases} v^{1,R_j}(x) + \left(\frac{L}{H}x_2 - \frac{L}{2}, 0\right) & x \in R_j, \, 0 \le j \le j_0, \\ w(x) & \text{otherwise.} \end{cases}$$

Reasoning symmetrically we obtain a construction on the whole domain Ω. As usual we will denote with χ the projection of ∇u onto K_0.

Step 5: Energetic cost and optimization of parameters. By symmetry we can restrict to computing the total energy on T. Splitting the contributions on R_j and $T \setminus T_0$ we obtain

$$\hat{E}(u, \chi) \lesssim \int_{T \setminus T_0} \mathrm{dist}^2(\nabla w, K_0) \mathrm{d}x + |D\chi|(T \setminus T_0)$$

$$+ \sum_{j=0}^{j_0} \Big(\int_{R_j} \mathrm{dist}^2 \Big(\nabla v^{1,R_j} + \frac{L}{H} e_1 \otimes e_2, K_0 \Big) \mathrm{d}x + |D\chi^{1,R_j}|(R_j) \Big).$$

$$(33)$$

We study the two contributions on the right-hand side of (33) separately, starting from the energy contribution in $T \setminus T_0$.

The term $|D\chi|(T \setminus T_0)$ is proportional to the perimeter of Ω, hence $|D\chi|(T \setminus T_0) \lesssim H$. We now need to control the measure of $T \setminus T_0$. This consists of the union of triangles of (orthogonal) sides r_j and $\frac{L}{H} r_j$ for $j \in \{0, \ldots, j_0\}$ and one of (orthogonal) sides $\frac{H}{2} - h_{j_0+1}$ and $\frac{L}{H}(\frac{H}{2} - h_{j_0+1})$ (see Fig. 4). Recalling that, by definition of h_{j_0}, $\frac{H}{2} - h_{j_0+1} \leq \frac{L}{2}$, we obtain the following estimate

$$|T \setminus T_0| \lesssim r^2 \frac{L}{H} \sum_{j \geq 0} \Big(1 - \frac{2}{H} r \Big)^{2j} + \frac{L^3}{H} \lesssim rL + \frac{L^3}{H}.$$

From this and the fact that $\mathrm{dist}(\nabla w, K_0) \lesssim 1$, we obtain

$$\int_{T \setminus T_0} \mathrm{dist}^2(\nabla w, K_0) \mathrm{d}x + |D\chi|(T \setminus T_0) \lesssim rL + \frac{L^3}{H} + H. \qquad (34)$$

We analyze the energy contributions originating from the rectangles R_j in (33). Since the matrix $\frac{L}{H} e_1 \otimes e_2$ does not affect the projection of $\nabla v^{1,R_j}$ onto K_0, from (31) for every j we have

$$\int_{R_j} \mathrm{dist}^2 \Big(\nabla v^{1,R_j} + \frac{L}{H} e_1 \otimes e_2, K_0 \Big) \mathrm{d}x + |D\chi^{1,R_j}|(R_j) \lesssim \frac{r_j^3}{\ell_j} + |R_j| \frac{L^2}{H^2} + \ell_j.$$
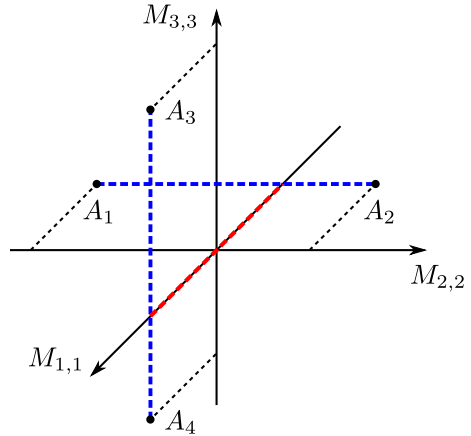
By summing over j we obtain

$$\sum_{j=0}^{j_0} \Big(\int_{R_j} \mathrm{dist}^2 \Big(\nabla v^{1,R_j} + \frac{L}{H} e_1 \otimes e_2, K_0 \Big) \mathrm{d}x + |D\chi^{1,R_j}|(R_j) \Big)$$

$$\lesssim \sum_{j \geq 0} \Big(\frac{r^3}{L} \Big(1 - \frac{2}{H} r \Big)^{2j} + L \Big(1 - \frac{2}{H} r \Big)^j \Big) + |T| \frac{L^2}{H^2} \lesssim r^2 \frac{H}{L} + \frac{HL}{r} + \frac{L^3}{H}.$$

$$(35)$$

Inserting (34) and (35) into (33) we infer that

$$\hat{E}(u, \chi) \lesssim rL + H + \frac{L^3}{H} + r^2 \frac{H}{L} + \frac{HL}{r}. \qquad (36)$$

Fig. 5 The matrix set K defined in (37): In blue the set $K^{(1)} \setminus K$, in red $K^{(2)} \setminus K^{(1)}$

Optimizing the expression above in r and H we get $r \sim L^{\frac{2}{3}}$ and $H \sim L^{\frac{4}{3}}$. Notice that the choice $r \sim L^{\frac{2}{3}}$ is compatible with the condition $\ell > 4h$ on rectangles R of Step 2 (which for $R = R_j$ corresponds to $\ell_j > 4r_j$) and therefore the construction above is well-defined. The relation $HL \sim V$ yields $L \sim V^{\frac{3}{7}}$, $H \sim V^{\frac{4}{7}}$, and the result follows.
□

5.3 A Three-Dimensional Analogue

An interesting three-dimensional modification of the previous setting is the following: We consider $K = \{A_1, A_2, A_3, A_4\} \subset \mathbb{R}^{3 \times 3}$ with

$$
A_1 = \begin{pmatrix} -1 & 0 & 0 \\ 0 & -2 & 0 \\ 0 & 0 & 0 \end{pmatrix}, \quad A_2 = \begin{pmatrix} -1 & 0 & 0 \\ 0 & 1 & 0 \\ 0 & 0 & 0 \end{pmatrix}, \quad A_3 = \begin{pmatrix} 1 & 0 & 0 \\ 0 & 0 & 0 \\ 0 & 0 & 2 \end{pmatrix}, \quad A_4 = \begin{pmatrix} 1 & 0 & 0 \\ 0 & 0 & 0 \\ 0 & 0 & -1 \end{pmatrix}. \tag{37}
$$

First-order laminates are the segments $K^{(1)} = \text{conv}(A_1, A_2) \cup \text{conv}(A_3, A_4)$, whereas the second-order laminates consist of

$$
K^{(2)} \setminus K^{(1)} = \left\{ \begin{pmatrix} \mu & 0 & 0 \\ 0 & 0 & 0 \\ 0 & 0 & 0 \end{pmatrix} : |\mu| < 1 \right\}
$$

which in particular contains **0**, as can be seen in Fig. 5.

In this case we have $\chi_{1,1} = -\chi_1 - \chi_2 + \chi_3 + \chi_4$, $\chi_{2,2} = -2\chi_1 + \chi_2$ and $\chi_{3,3} = 2\chi_3 - \chi_4$, and therefore we have the nonlinear relation

$$
\chi_{1,1} = g(\chi_{2,2} + \chi_{3,3}) \tag{38}
$$

with g a polynomial. Because of the structure of the wells, we can choose g to be the same polynomial as in (25).

For this setting, working analogously as done for the two-dimensional case, we have the following lower scaling bounds.

Proposition 5.3 *Let $\hat{E}(V)$ be as in (12) and let K be as in (37). Then there exists a positive constant $C > 0$ depending on K such that for every $V > 0$ there holds*

$$C\hat{r}(V) \le \hat{E}(V), \quad \text{where} \quad \hat{r}(V) = \begin{cases} V^{\frac{2}{3}} & \text{if } V \le 1, \\ V^{\frac{9}{11}} & \text{if } V > 1. \end{cases} \tag{39}$$

Moreover, for every $\epsilon > 0$ there holds

$$Cr_\epsilon(V) \le E_\epsilon(V), \quad \text{where} \quad r_\epsilon(V) = \begin{cases} \epsilon V^{\frac{2}{3}} & \text{if } V \le \epsilon^3, \\ \epsilon^{\frac{6}{11}} V^{\frac{9}{11}} & \text{if } V > \epsilon^3. \end{cases} \tag{40}$$

We remark that the lower scaling bound in (39) and (40) is the same as the one obtained in Knüpfer et al. (2013) in the case of nucleation for the geometrically linearized cubic-to-tetragonal phase transition. In the geometrically linearized cubic-to-tetragonal phase transition the zero matrix also is a second-order laminate. The geometrically linearized cubic-to-tetragonal phase transition includes a geometrically linearized version of frame-indifference and thus $Skew(3)$-invariance. While our simplified model does not include this, it is rich enough to provide the same lower bound scaling behaviour. It could thus serve as a model problem in which one can possibly study finer properties of this phase transformation.

We expect that upper-bound constructions matching the lower-scaling bounds can be obtained working analogously as in Knüpfer et al. (2013, Sect. 6). Since this is not the main goal of our work we omit to study it.

Proof The lower bound is proved analogously as done in the two-dimensional case. Let $0 < \mu < 1$, $\mu_2, \mu_3 > 0$ be as in the proof of Proposition 5.1. From Lemmas 2.4–2.6 and relation (25) we have

$$V \le C\mu^2\mu_3^3 V^2 + C_\gamma(\mu^{-2} + \mu_2^{-1})\psi_\gamma\big(\hat{E}(\chi)\big).$$

Again, from Remark 2.2 $\hat{E}(\chi) \gtrsim 1$. Thus, by fixing γ, from the inequality above we obtain

$$V \lesssim \mu^2\mu_3^3 V^2 + (\mu^{-2} + \mu_2^{-1})\hat{E}(\chi).$$

Since $\mu_3 \sim \mu\mu_2$, we choose μ_2 sufficiently small such that $\mu^5\mu_2^3 V^2 \sim V$, that is $\mu_2 \sim V^{-\frac{1}{3}}\mu^{-\frac{5}{3}}$. This implies

$$V \lesssim (\mu^{-2} + V^{\frac{1}{3}}\mu^{\frac{5}{3}})\hat{E}(\chi).$$

Optimizing, we choose $\mu \sim V^{-\frac{1}{11}}$ and therefore obtain

$$V \lesssim V^{\frac{2}{11}}\hat{E}(\chi),$$

which gives the claim.

As above, the ϵ-scaling behaviour follows by rescaling as in Sect. 2.2. $\qquad\square$

6 A Third-Order Laminate: The 8+1-Wells Case

In this section, we provide the proof of Proposition 1.2. As in the previous sections, it suffices to deduce the non-dimensionalized bounds. These read as follows:

Proposition 6.1 *Let $\hat{E}(V)$ be as in (12) and let K be as in (7). Then, there exists a positive constant $C > 0$ depending on K such that for every $V > 0$ it holds*

$$\hat{E}(V) \geq C\hat{r}(V), \text{ where } \hat{r}(V) = \begin{cases} V^{\frac{2}{3}}, & V \leq 1, \\ V^{\frac{6}{7}}, & V > 1. \end{cases}$$

The main idea of the argument consists in using that $\chi_{1,1}$ determines $\chi_{2,2}$, $\chi_{3,3}$ and that $\chi_{2,2}$ determines $\chi_{3,3}$. Thus, an iterated commutator estimate as in Sect. 2 is possible, and an optimization argument yields the lower bound.

Proof We argue in several steps. As a preliminary observation, we note that it suffices to prove the bounds for $V > 1$ since the small volume setting is a direct consequence of the isoperimetric inequality, see Sect. 2.3.

Step 1: First energy bounds. From Lemma 2.4 we directly obtain that for $\mu_2, \mu \in (0, 1)$ to be fixed it holds that

$$\sum_{j=1}^{3} \|\chi_{j,j} - \chi_{j,\mu,\mu_2}(D)\chi_{j,j}\|_{L^2}^2 \leq C(\mu^{-2}E_{el}(\chi) + \mu_2^{-1}E_{\text{surf}}(\chi)). \quad (41)$$

Step 2: $\chi_{1,1}$ determines $\chi_{2,2}$ and $\chi_{3,3}$. From the structure of the wells, we observe that $\chi_{2,2} = f_{1,2}(\chi_{1,1})$ and $\chi_{3,3} = f_{1,3}(\chi_{1,1})$ for some polynomials $f_{1,2}, f_{1,3}$ (see Remark 6.2 for an explicit example). As a consequence, we may invoke Lemma 2.5 which, combined with (41), yields that for $0 < \mu_3 = M\mu\mu_2 < \mu_2$ and for $j \in \{2, 3\}$ (where we have possibly reduced the value of μ if needed), it holds that

$$\|\chi_{j,j} - \chi_{j,\mu,\mu_3}(D)\chi_{j,j}\|_{L^2}^2 \leq C\psi_{\gamma}\left(\|\chi_{1,1} - \chi_{1,\mu,\mu_2}(D)\chi_{1,1}\|_{L^2}^2\right) \\ + C(\mu^{-2}E_{el}(\chi) + \mu_2^{-1}E_{\text{surf}}(\chi)).$$

Moreover, due to Remark 2.2 and analogously as in the proof of Proposition 5.1, we may drop the function ψ_{γ}, which yields, again from (41), that

$$\|\chi_{j,j} - \chi_{j,\mu,\mu_3}(D)\chi_{j,j}\|_{L^2}^2 \leq C(\mu^{-2}E_{el}(\chi) + \mu_2^{-1}E_{\text{surf}}(\chi)), \quad j \in \{2, 3\}. \quad (42)$$

Step 3: $\chi_{2,2}$ determines $\chi_{3,3}$. Using that $\chi_{3,3} = f_{2,3}(\chi_{2,2})$ with $f_{2,3}$ a polynomial (see Remark 6.2), we again invoke Lemma 2.5 with $\mu' = \mu_2$, $\mu'' = \mu_3$ and $\tilde{\mu} = \mu_4$.

Hence, for $0 < \mu_4 = M\mu\mu_3 < \mu_3$ this yields the bounds

$$
\begin{aligned}
\|\chi_{3,3} - \chi_{3,\mu,\mu_4}(D)\chi_{3,3}\|_{L^2}^2 &\le C\psi_\gamma\big(\|\chi_{2,2} - \chi_{2,\mu,\mu_3}(D)\chi_{2,2}\|_{L^2}^2\big) \\
&\quad + C(\mu^{-2}E_{el}(\chi) + \mu_2^{-1}E_{\text{surf}}(\chi)) \\
&\le 2C(\mu^{-2}E_{el}(\chi) + \mu_2^{-1}E_{\text{surf}}(\chi)),
\end{aligned}
$$

where the last inequality is a consequence of (42).

Step 4: Optimization and conclusion. With the bounds from the previous steps, we conclude that

$$
\begin{aligned}
V &= \|\chi_{33}\|_{L^2}^2 \\
&\le 2(\|\chi_{3,\mu,\mu_4}(D)\chi_{3,3}\|_{L^2}^2 + \|\chi_{3,3} - \chi_{3,\mu,\mu_4}(D)\chi_{3,3}\|_{L^2}^2) \\
&\lesssim \mu^2\mu_4^3 V^2 + (\mu_2^{-1} + \mu^{-2})\hat{E}(\chi) \sim \mu^2(\mu^2\mu_2)^3 V^2 + (\mu_2^{-1} + \mu^{-2})\hat{E}(\chi).
\end{aligned}
\tag{43}
$$

Absorbing the first right-hand contribution from (43) into the left-hand side, we choose $\mu_2 \sim \mu^{-\frac{8}{3}}V^{-\frac{1}{3}}$. As a consequence, inserting this back into (43), we arrive at

$$
V = \|\chi_{3,3}\|_{L^2}^2 \lesssim (\mu^{\frac{8}{3}}V^{\frac{1}{3}} + \mu^{-2})\hat{E}(\chi).
$$

Choosing $\mu \sim V^{-\frac{1}{14}}$, we obtain that

$$
V \lesssim V^{\frac{1}{7}}\hat{E}(\chi),
$$

which yields the claim. $\qquad\square$

Remark 6.2 We provide examples of nonlinear polynomials such that

$$
\chi_{2,2} = f_{1,2}(\chi_{1,1}), \quad \chi_{3,3} = f_{1,3}(\chi_{1,1}), \quad \chi_{3,3} = f_{2,3}(\chi_{2,2}).
\tag{44}
$$

These can be found for instance by interpolation. Hence, defining the numerical constants $a = 1344, b = 1440, c = 576, d = 5040$, the polynomials

$$
\begin{aligned}
f_{1,2}(t) &= -\frac{1}{a}t^8 + \frac{11}{b}t^6 + \frac{83}{c}t^4 - \frac{5801}{d}t^2, \\
f_{1,3}(t) &= 5\Big(\frac{1}{a}t^8 - \frac{31}{b}t^6 + \frac{101}{c}t^4 - \frac{1787}{d}t^2\Big), \\
f_{2,3}(t) &= \frac{5}{12}t^4 - \frac{17}{12}t^2,
\end{aligned}
$$

comply with (44).

7 An Infinite-Order Laminate: Setting for the Tartar case

As a last but not least example, we turn to the proof of Theorem 4. Here the phase indicator χ has the form

$$\chi = \begin{pmatrix} -\chi_1 + \chi_3 - 3\chi_2 + 3\chi_4 & 0 \\ 0 & -3\chi_1 + 3\chi_3 + \chi_2 - \chi_4 \end{pmatrix}$$

with $\chi_j \in BV(\mathbb{R}^2; \{0, 1\})$ with $\chi_1 + \chi_2 + \chi_3 + \chi_4 \leq 1$. For this structure of the energy wells each component $\chi_{j,j}$ determines the other by a nonlinear polynomial relation

$$\chi_{1,1} = f(\chi_{2,2}) \quad \text{and} \quad \chi_{2,2} = g(\chi_{1,1}). \tag{45}$$

This is a consequence of the rank-one-incompatibility of K, for a detailed treatment see Rüland and Tribuzio (2022).

After non-dimensionalization it suffices to prove the following estimates:

Theorem 8 *Let $\hat{E}(V)$ be as in (12) and let K be as in (8). Then there exist four positive constants $C^{(1)} > C^{(2)} > 0$, $C_2 > C_1 > 0$ depending on K such that for every $V > 0$ there holds*

$$C_1 \hat{r}^{(1)}(V) \leq \hat{E}(V) \leq C_2 \hat{r}^{(2)}(V), \quad \text{where} \quad \hat{r}^{(j)}(V) = \begin{cases} V^{\frac{1}{2}} & \text{if } V \leq 1, \\ V \exp(-C^{(j)}(\log(V))^{\frac{1}{2}}) & \text{if } V > 1. \end{cases} \tag{46}$$

Similarly as in the previous sections, we split this into an upper bound construction and lower bound estimates which we provide in the next subsections.

7.1 Upper Bounds

We begin by providing an upper bound construction:

Proposition 7.1 *Let $\hat{E}(u, \chi)$ be as in (11) and let K be as in (8). Let $V > 1$ be given and let $\Omega = [0, L] \times [0, H]$ with $H \leq L$ and $HL = V$. There are two universal constants $0 < c < 1$, $C > 0$ such that for every L, H as above for which*

$$L \exp\left(-C(\log(L))^{\frac{1}{2}}\right) < cH, \tag{47}$$

holds, there exist $u \in W_0^{1,\infty}(\Omega; \mathbb{R}^2)$ and $\chi \in BV(\mathbb{R}^2; K_0)$ with $\mathrm{supp}(\chi) = \Omega$ such that

$$\hat{E}(u, \chi) \lesssim V \exp\left(-C^{(2)}(\log(V))^{\frac{1}{2}}\right)$$

for every constant $0 < C^{(2)} \leq (\log(2))^{\frac{1}{2}}$.

The argument for this relies on a quantitative (in the volume) analysis of the constructions from Chipot (1999), Rüland and Tribuzio (2022), Winter (1997).

Proof Let $r > 0$ be a parameter to be determined, depending on L and H and complying with

$$r < c_0 H, \quad \text{for some universal constant } c_0 < 1. \tag{48}$$

For such r we define the following construction: Consider $r_j > 0$ for $j \in \mathbb{N}$, $j \geq 2$, such that $r_{j+1} < r_j$ and $r_2 < r$. Here, we assume that r_j can be expressed in terms of r. Let $u_{r,k}$ be obtained via the k-th-order lamination construction defined in Step 1 of the proof of Winter (1997, Theorem 3.1) (see also Rüland and Tribuzio 2022, Sect. 2). Using the notation of Rüland and Tribuzio (2022) we also take $\chi_{r,k}$ to be the projection of $\nabla u_{r,k}$ onto K_0. In Winter (1997) (equation at page 17 with $\epsilon = 1$) it is proved that

$$\hat{E}(u_{r,k}, \chi_{r,k}) \lesssim LH\Big(\frac{1}{2^k} + \frac{r}{L} + \sum_{j=2}^{k} 2^{-j}\frac{r_j}{r_{j-1}} + 2^{-j}\frac{1}{r_k}\Big). \tag{49}$$

The same estimate can be found by reworking the lines of Rüland and Tribuzio (2022) as well. A good choice for the length scales r_j comes from an optimization procedure; by imposing $\frac{r}{L} \sim \frac{r_j}{r_{j-1}}$ we get $r_j \sim \frac{r^j}{L^{j-1}}$. With this choice (49) reduces to

$$\hat{E}(u_{r,k}, \chi_{r,k}) \lesssim H\big(L2^{-k} + r + L^k r^{-k}\big).$$

Optimizing r in terms of k and L leads to $r \sim L^{\frac{k}{k+1}}$. A further optimization argument in k implies $2^k \sim L^{\frac{1}{k+1}}$, which is nontrivial since $L > 1$. This finally results in the choice $k \sim \log(L)^{\frac{1}{2}}$.

In order to obtain information on the constant $C^{(2)}$, we let $u := u_{\hat{r},\hat{k}}$ and $\chi := \chi_{\hat{r},\hat{k}}$ with

$$\hat{k} + 1 = \lfloor c_1(\log(L))^{\frac{1}{2}} \rfloor \quad \text{and} \quad \hat{r} = c_2 L^{\frac{\hat{k}}{\hat{k}+1}} \leq c_2 L \exp\big(-c_1^{-1}(\log(L))^{\frac{1}{2}}\big),$$

for some constants $c_1, c_2 > 0$. We observe that condition (47) implies (48) if $c < c_2^{-1}c_0$ and $C \leq c_1^{-1}$.

After optimization, since $L^{\hat{k}}\hat{r}^{-\hat{k}} = \hat{r}$ we have

$$\hat{E}(u, \chi) \lesssim H(\hat{r} + L2^{-\hat{k}}) \lesssim HL\Big(\exp\big(-c_1\log(2)(\log(L))^{\frac{1}{2}}\big) + \exp\big(-c_1^{-1}(\log(L))^{\frac{1}{2}}\big)\Big).$$

By the arbitrary choice of the constant c_1 in the definition of $\hat{k}$, a final optimization of the right-hand side implies $c_1 = (\log(2))^{-\frac{1}{2}}$ from which we conclude the result. □

Remark 7.2 We highlight that the condition (47) can be viewed as a geometric information on the inclusion domains, in the sense that (scaling) optimal realizations of the type discussed above cannot be too thin.

Remark 7.3 (*Towards a better constant*) In the case of a fixed domain with $V \sim 1$ in Winter (1997) an upper scaling bound of form

$$E_\epsilon(V) \lesssim \exp\left(-\sigma|\log(\epsilon)|^{\frac{1}{2}}\right)$$

with $\sigma \in (0, (2\log(2))^{\frac{1}{2}})$ was proved. This was possible thanks to a finer optimization argument on the length scales r_j with respect to the one performed in the proof above. We believe that reworking our construction in the same way would imply the upper bound of Proposition 7.1 to be true for every $0 < C^{(2)} < (2\log(2))^{\frac{1}{2}}$. Nonetheless, this may not be the optimal range of $C^{(2)}$, since iterated branching-type constructions produce intermediate steps that have smaller (in terms of scaling) energy than (49). It thus remains an interesting problem to determine the optimal constants $C^{(1)}$, $C^{(2)}$ in the subalgebraic scaling law from Proposition 7.1.

7.2 Lower Bounds

We complement the upper bound construction with an ansatz-free lower bound estimate.

Proposition 7.4 *Let $\hat{E}(V)$ be as in (12) and let K be as in (8). Then for every $V > 1$ there holds*

$$\hat{E}(V) \gtrsim V \exp\left(-C^{(1)}(\log(V))^{\frac{1}{2}}\right),$$

for some constant $C^{(1)} > (2\log(96))^{\frac{1}{2}}$.

Proof As in Rüland and Tribuzio (2022), we first observe that since the $\chi_{1,1}$ component determines the $\chi_{2,2}$ component and vice versa by (45), we can iterate the commutator bounds of Lemma 2.5. This yields that there exists a constant $C > 0$ such that for any $m \in 2\mathbb{N}$ it holds that

$$
\begin{aligned}
V &\lesssim \|(\chi_{1,\mu,\mu_m}(D) + \chi_{2,\mu,\mu_{m+1}}(D))\chi\|_{L^2}^2 + \|\chi_{1,\mu,\mu_m}(D)\chi_{1,1} - \chi_{1,1}\|_{L^2}^2 \\
&\quad + \|\chi_{2,\mu,\mu_{m+1}}(D)\chi_{2,2} - \chi_{2,2}\|_{L^2}^2 \\
&\lesssim \mu\mu_m^2 V^2 + C^m(\mu^{-2} + \mu_2^{-1})\hat{E}(\chi),
\end{aligned}
$$

where $0 < \mu, \mu_2 < 1$ are parameters to be determined and $\mu_m := c^m \mu^{m-2}\mu_2 < \mu_{m-1}$ for some constant $c > 1$. Here we have already used that, by the assumption that $V \geq 1$ and Remark 2.2, we do not have losses due to the fact that $\hat{E}(\chi) \gtrsim 1$. In particular, we may consider the commutator with some γ fixed and still the leading term is the linear one. From definition of μ_m we have

$$V \lesssim c^{2m}\mu^{2m-3}\mu_2^2 V^2 + C^m(\mu^{-2} + \mu_2^{-1})\hat{E}(\chi).$$

From $V \sim c^{2m} \mu^{2m-3} \mu_2^2 V^2$ we infer $\mu_2 \sim V^{-\frac{1}{2}} c^{-m} \mu^{-\frac{2m-3}{2}}$ which gives

$$V \lesssim C_0^m (\mu^{-2} + \mu^{\frac{2m-3}{2}} V^{\frac{1}{2}}) \hat{E}(\chi)$$

with $C_0 > Cc$. An optimization, i.e. the choice $\mu \sim V^{-\frac{1}{2m+1}}$, leads to

$$V \lesssim C_0^m V^{\frac{2}{2m+1}} \hat{E}(\chi).$$

Optimizing the right-hand side by taking $m \in 2\mathbb{N}$ such that $C_0^m \sim V^{\frac{2}{2m+1}}$, which gives $m \sim (\log(C_0))^{-\frac{1}{2}} (\log(V))^{\frac{1}{2}}$, we obtain

$$V \exp(-2(\log(C_0))^{\frac{1}{2}} \log(V)^{\frac{1}{2}}) \lesssim \hat{E}(\chi).$$

In the end, in order to obtain information on the constant $C^{(1)}$ we make use of estimates on the constants C and c that have been obtained in Rüland and Tribuzio (2022). To be precise, since we can choose f and g in formula (45) to be polynomials of degree 3 from Rüland and Tribuzio (2022, formulas (30) and (34)), the above argument remains valid for $c = 12$. Moreover, constant C above is made explicit in Rüland and Tribuzio (2022, formula (35)), in particular $C > 8$. Hence, the proof is complete.   □

8 Conclusion

Finally, concluding our article, we briefly summarize our main findings. Seeking to contribute to an improved understanding of the complexity of microstructures in non-convex, highly anisotropic, nonlocal, vectorial singular perturbation problems as arising, for instance, in the modelling of nucleation phenomena in shape-memory alloys, in this article

- we have identified non-convex, highly anisotropic models (in the form of the sets K_0) in which the complexity of the associated scaling law is determined by the *order of lamination* of the parent phase with respect to the nucleating phase;
- to this end, in proving lower bounds, we have made systematic use of commutator bounds and "nonlinear structural properties" of the sets K_0;
- and have illustrated that—while being strongly simplified in that frame-indifference and the associated gauges are neglected—in interesting situations (e.g. as outlined in Proposition 5.3) our models recover scaling laws which had been earlier deduced in the physically relevant settings *with* gauges.

We emphasize that, in particular, these simplified models may thus be considered as interesting substitutes for some more realistic models with gauges. Thus, one may hope to possibly infer interesting, finer information on the more complex models by further studying these simplified substitutes.

In addition to these observations, let us however reiterate that for general nucleation problems the order of lamination is *not* the only parameter determining the scaling

law behaviour. For instance, we expect rather different behaviour for the "stair-case laminates" from Conti et al. (2005) and Rüland and Tribuzio (2021). We further hope that the ideas from the present article are also of interest in settings of geometrically linearized elasticity and that the systematic commutator estimates may also play a useful role in such a more complicated context.

Data Availability Data sharing not applicable to this article as no datasets were generated or analysed during the current study.

Declarations

Conflict of interest The authors have no conflict of interest to declare that are relevant to the content of this article.

Research Involving Human Participants and/or Animals Not applicable.

Informed Consent Not applicable.

Appendix A. Branching Constructions in Rectangular Domains

In this section we present branching constructions as alternatives to the diamond-shaped constructions from Propositions 4.2 and 5.2 and step 2 of the proof of Corollary 1.1.

A.1. A Branching Construction for the Upper Bound from Theorem 6

We begin by presenting the branching construction for the upper bound from Theorem 6. To do so we refer to Rüland and Tribuzio (2021, Lemma 3.2) which in turn reworks (Chan and Conti 2015, Lemma 2.3):

Alternative proof of Proposition 4.2 Given $H > L > 1$ consider the rectangle $\Omega = [0, L] \times [0, H]$ and consider the construction given by Rüland and Tribuzio (2021, Lemma 3.2) for the domain Ω and corresponding to $N = \lceil \frac{4L}{H} \rceil$, where $\lceil \cdot \rceil$ denotes

the upper integer-part. For a better understanding, we recall that N represents the number of changes of phase of the zeroth generation of the branching construction. From formula (19) of Rüland and Tribuzio (2021, Lemma 3.2) with $p = 2$ and $\epsilon = 1$ we get

$$\hat{E}(u, \chi) \leq C\Big(\frac{L^3}{H} + H\Big), \tag{50}$$

where χ is the projection of ∇u onto K_0 and $C > 0$ is a positive constant depending on K. Notice also that $1 \leq N \leq 4$ and thus its contribution in (19) of Rüland and Tribuzio (2021, Lemma 3.2) is absorbed by the constant C in the inequality above. By an optimization argument we obtain $L \sim H^{\frac{2}{3}}$ which implies $V = H^{\frac{5}{3}}$ and the result follows. □

A.2 A Branching Construction for the Upper Bound from Corollary 1.1

We complement the higher-dimensional lens-shaped upper bound construction from the proof of Corollary 1.1 with the corresponding branching construction.

Alternative proof of the upper bound construction from Corollary 1.1 We follow a similar construction as in the first-order outer laminate from Rüland and Tribuzio (2021, Proposition 6.3). Let $u : \mathbb{R}^2 \to \mathbb{R}^2$ be the functions introduced in the alternative proof of Proposition 4.2 in the previous Sect. A.1. Then, we consider $\Omega = [0, L] \times [0, H]^{n-1}$ and define $\tilde{u}(x_1, x_2, \ldots, x_n) = (u(x_1, \rho(x_2, \ldots, x_n)), 0, \ldots, 0)$ with

$$\rho(x_2, \ldots, x_n) = \max_{2 \leq j \leq n-1} \Big\{\Big|x_j - \frac{H}{2}\Big|\Big\} + \frac{H}{2},$$

and let $\tilde{\chi}$ be the projection of $\nabla \tilde{u}$ onto K_0. Hence (50) gives

$$\hat{E}(\tilde{u}, \tilde{\chi}) \lesssim \Big(\frac{L^3}{H} + H\Big)H^{n-2}.$$

By optimization we obtain that $L \sim H^{\frac{2}{3}}$. Hence, the constraint $LH^{n-1} = V$ yields $H \sim V^{\frac{3}{3n-1}}$ and thus the desired result. □

A.3 A Branching Construction for the Upper Bound from Theorem 7

In addition to the lens-shaped construction from the proof of Theorem 7 which was presented in the main body of the text, an alternative upper bound construction for Theorem 7 can be realized by a double branching construction, where the coarsest oscillation happens a number of times of the order of one. The construction retraces the steps of Rüland and Tribuzio (2021, Sect. 5) keeping track of H and L (that are constants there).

Proof of Proposition 5.2 by means of a double branching construction As a first step we consider the construction given in the alternative proof of Proposition 4.2 in Sect. A.1.

In particular, as in the alternative proof of Proposition 4.2 in Sect. A.1, we apply the construction from Rüland and Tribuzio (2021, Lemma 3.2) with the following gradients

$$B_1 = \frac{1}{3}A_1 + \frac{2}{3}A_2 \quad \text{and} \quad B_2 = \frac{1}{3}A_3 + \frac{2}{3}A_4$$

(i.e. where in the notation from Rüland and Tribuzio (2021, Lemma 3.2) $\{A, B\} = \{B_1, B_2\}$). We denote this macroscopic construction with $\tilde{u}$ and $\tilde{\chi}$.

As in the aforementioned proof, the number of oscillations of the zeroth generation of the branching construction (loosely speaking the number of "trees") is $1 \leq N \leq 4$. Thus, without loss of generality, we assume that we have only one tree of branching, i.e., $N = 1$.

We briefly describe the construction for the sake of clarity of exposition: again consider $\Omega = [0, L] \times [0, H]$ with $H > L > 1$. This domain is subdivided in 2^j identical cells equal (up to horizontal translation) to $[0, \ell_j] \times [h_j, h_{j+1}]$ for every $j \geq 0$ corresponding to the generation. This process stops when j is such that $\ell_j > h_j$, then using a cut-off argument to match the austenite phase. Here $\ell_j = L2^{-j}$ and $h_j = \frac{H}{2}\theta^j$ for some $\theta \in (\frac{1}{4}, \frac{1}{2})$. In each cell $\tilde{u}$ is defined by Rüland and Tribuzio (2021, Lemma 3.1) with $A = B_1$ and $B = B_2$.

Now we build u and χ replacing $\tilde{u}$ and $\tilde{\chi}$ with a branching construction, having gradients A_1, A_2 on $\{\tilde{\chi} = B_1\}$ and A_3, A_4 on $\{\tilde{\chi} = B_2\}$, respectively. For each generation the set $\{\tilde{\chi} = B_1\}$ consists (up to translation) of $R_j \cup \varphi(R_j)$ where

$$R_j = \left[0, \frac{\ell_j}{4}\right] \times [0, h_j] \quad \text{and} \quad \varphi(x_1, x_2) = \left(\frac{\ell_j x_2}{4h_j}, x_2\right).$$

In each rectangle R_j we apply Rüland and Tribuzio (2021, Lemma 3.2) with $p = 2$ and $\epsilon = 1$ (inverting the roles of x_1 and x_2); its energy contribution is

$$(2\theta^3)^j \frac{H^3}{N_j^2 L} + 2^{-j} L N_j.$$

The shear gives an additional elastic energy term of order $(\frac{\ell_j}{h_j})^2 h_j \ell_j$ thus, the contribution in $R_j \cup \varphi(R_j)$ is

$$(2\theta^3)^j \frac{H^3}{N_j^2 L} + 2^{-j} L N_j + \frac{\ell_j^3}{h_j}.$$

We refer the interested reader to Rüland and Tribuzio (2021) for details, in particular, see the first formula above (43) on page 29 there. An optimization argument gives $N_j \sim HL^{-\frac{2}{3}}(\theta 2^{\frac{2}{3}})^j$. The construction on $\{\tilde{\chi} = B_2\}$ is completely analogous. Multiplying by the number of cells 2^j at the jth refinement generation and summing over j we

infer

$$\hat{E}(u, \chi) \lesssim \sum_{j=0}^{\infty} (\theta 2^{\frac{2}{3}})^j (HL^{\frac{1}{3}}) + (\theta^{-1} 2^{-2})^j \frac{L^3}{H} \lesssim HL^{\frac{1}{3}} + \frac{L^3}{H}.$$

By another optimization argument we choose $L \sim H^{\frac{3}{4}}$ which implies (from the volume constraint) that $L \sim V^{\frac{3}{7}}$, $H \sim V^{\frac{4}{7}}$, and the result follows. □

References

Akramov, I., Knüpfer, H., Kružik, M., Rüland, A.: Minimal energy for geometrically nonlinear elastic inclusions in two dimensions. arXiv preprint arXiv:2207.13746 (2022)

Aumann, R.J., Hart, S.: Bi-convexity and bi-martingales. Isr. J. Math. **54**(2), 159–180 (1986)

Ball, J.M.: A version of the fundamental theorem for Young measures. In: PDEs and Continuum Models of Phase Transitions. Springer, pp. 207–215 (1989)

Ball, J.M., James, R.D.: Fine phase mixtures as minimizers of energy. In: Analysis and Continuum Mechanics. Springer, pp. 647–686 (1989)

Ball, J.M., James, R.D.: Proposed experimental tests of a theory of fine microstructure and the two-well problem. Philos. Trans. R. Soc. Lond. A **338**(1650), 389–450 (1992)

Ball, J.M., Koumatos, K.: Quasiconvexity at the boundary and the nucleation of austenite. Arch. Ration. Mech. Anal. **219**(1), 89–157 (2016)

Bella, P., Goldman, M.: Nucleation barriers at corners for a cubic-to-tetragonal phase transformation. Proc. R. Soc. Edinb. Sect. A Math. **145**(4), 715–724 (2015)

Bhattacharya, K., Kohn, R.V.: Elastic energy minimization and the recoverable strains of polycrystalline shape-memory materials. Arch. Ration. Mech. Anal. **139**(2), 99–180 (1997)

Capella, A., Otto, F.: A rigidity result for a perturbation of the geometrically linear three-well problem. Commun. Pure Appl. Math. **62**(12), 1632–1669 (2009)

Capella, A., Otto, F.: A quantitative rigidity result for the cubic-to-tetragonal phase transition in the geometrically linear theory with interfacial energy. Proc. R. Soc. Edinb. Sect. A Math. **142**, 273–327 (2012). https://doi.org/10.1017/S0308210510000478

Casadio-Tarabusi, E.: An algebraic characterization of quasi-convex functions. Ricerche Mat **42**(1), 11–24 (1993)

Cesana, P., Della Porta, F., Rüland, A., Zillinger, C., Zwicknagl, B.: Exact constructions in the (non-linear) planar theory of elasticity: from elastic crystals to nematic elastomers. Arch. Ration. Mech. Anal. **237**(1), 383–445 (2020)

Chan, A., Conti, S.: Energy scaling and domain branching in solid–solid phase transitions. In: Singular Phenomena and Scaling in Mathematical Models. Springer, pp. 243–260 (2014)

Chan, A., Conti, S.: Energy scaling and branched microstructures in a model for shape-memory alloys with $SO(2)$ invariance. Math. Models Methods Appl. Sci. **25**(06), 1091–1124 (2015)

Chipot, M.: The appearance of microstructures in problems with incompatible wells and their numerical approach. Numer. Math. **83**(3), 325–352 (1999)

Chaudhuri, N., Müller, S.: Rigidity estimate for two incompatible wells. Cal. Var. **19**, 379–390 (2004)

Chipot, M., Müller, S.: Sharp energy estimates for finite element approximations of non-convex problems. In: IUTAM Symposium on Variations of Domain and Free-Boundary Problems in Solid Mechanics, pp. 317–325. Springer (1999)

Choksi, R., Kohn, R.V., Otto, F.: Domain branching in uniaxial ferromagnets: a scaling law for the minimum energy. Commun. Math. Phys. **201**(1), 61–79 (1999)

Conti, S.: Branched microstructures: scaling and asymptotic self-similarity. Commun. Pure Appl. Math. **53**(11), 1448–1474 (2000)

Conti, S.: Quasiconvex functions incorporating volumetric constraints are rank-one convex. Journal de mathématiques pures et appliquées **90**(1), 15–30 (2008)

Conti, S., Zwicknagl, B.: Low volume-fraction microstructures in martensites and crystal plasticity. Math. Models Methods Appl. Sci. **26**(07), 1319–1355 (2016)

Conti, S., Faraco, D., Maggi, F.: A new approach to counterexamples to L^1 estimates: Korn's inequality, geometric rigidity, and regularity for gradients of separately convex functions. Arch. Ration. Mech. Anal. **175**(2), 287–300 (2005)

Conti, S., Diermeier, J., Zwicknagl, B.: Deformation concentration for martensitic microstructures in the limit of low volume fraction. Calc. Var. Partial Differ. Equ. **56**(1), 16 (2017a)

Conti, S., Klar, M., Zwicknagl, B.: Piecewise affine stress-free martensitic inclusions in planar nonlinear elasticity. Proc. R. Soc. A Math. Phys. Eng. Sci. **473**(2203), 20170235 (2017b)

Conti, S., Diermeier, J., Melching, D., Zwicknagl, B.: Energy scaling laws for geometrically linear elasticity models for microstructures in shape memory alloys. ESAIM Control Optim. Calc. Var. **26**, 115 (2020)

Grafakos, L.: Classical Fourier analysis, vol. 2. Springer, Berlin (2008)

Knüpfer, H., Kohn, R.V.: Minimal energy for elastic inclusions. Proc. R. Soc. A Math. Phys. Eng. Sci. **467**(2127), 695–717 (2011)

Knüpfer, H., Muratov, C.B.: On an isoperimetric problem with a competing nonlocal term I: the planar case. Commun. Pure Appl. Math. **66**(7), 1129–1162 (2013)

Knüpfer, H., Nolte, F.: Optimal shape of isolated ferromagnetic domains. SIAM J. Math. Anal. **50**(6), 5857–5886 (2018)

Knüpfer, H., Otto, F.: Nucleation barriers for the cubic-to-tetragonal phase transformation in the absence of self-accommodation. ZAMM J. Appl. Math. Mech. **99**(2), e201800179 (2019)

Knüpfer, H., Stantejsky, D.: Asymptotic shape of isolated magnetic domains. arXiv preprint arXiv:2201.02384 (2022)

Knüpfer, H., Kohn, R.V., Otto, F.: Nucleation barriers for the cubic-to-tetragonal phase transformation. Commun. Pure Appl. Math. **66**(6), 867–904 (2013)

Kohn, R.V., Müller, S.: Branching of twins near an austenite-twinned-martensite interface. Philos. Mag. A **66**(5), 697–715 (1992)

Kohn, R.V., Müller, S.: Surface energy and microstructure in coherent phase transitions. Commun. Pure Appl. Math. **47**(4), 405–435 (1994)

Kohn, R.V., Wirth, B.: Optimal fine-scale structures in compliance minimization for a uniaxial load. Proc. R. Soc. A Math. Phys. Eng. Sci. **470**(2170), 20140432 (2014)

Kohn, R.V., Wirth, B.: Optimal fine-scale structures in compliance minimization for a shear load. Commun. Pure Appl. Math. **69**(8), 1572–1610 (2016)

Lorent, A.: An optimal scaling law for finite element approximations of a variational problem with nontrivial microstructure. ESAIM Math. Model. Numer. Anal. **35**(5), 921–934 (2001)

Lorent, A.: The two-well problem with surface energy. Proc. R. Soc. Edinb. Sect. A Math. **136**(4), 795–805 (2006)

Maggi, F.: Sets of finite perimeter and geometric variational problems: an introduction to Geometric Measure Theory. Number 135 in Cambridge Studies in Advanced Mathematics. Cambridge University Press (2012)

Müller, S.: Variational models for microstructure and phase transitions. In: Calculus of Variations and Geometric Evolution Problems. Springer, pp. 85–210 (1999)

Muratov, C., Knüpfer, H.: On an isoperimetric problem with a competing nonlocal term II: the general case. Commun. Pure Appl. Math. **67**(12), 1974–1994 (2014)

Nesi, V., Milton, G.W.: Polycrystalline configurations that maximize electrical resistivity. J. Mech. Phys. Solids **39**(4), 525–542 (1991)

Niemann, R., Backen, A., Kauffmann-Weiss, S., Behler, C., Rößler, U.K., Seiner, H., Heczko, O., Nielsch, K., Schultz, L., Fähler, S.: Nucleation and growth of hierarchical martensite in epitaxial shape memory films. Acta Materialia **132**, 327–334 (2017)

Rüland, A.: A rigidity result for a reduced model of a cubic-to-orthorhombic phase transition in the geometrically linear theory of elasticity. J. Elast. **123**(2), 137–177 (2016)

Rüland, A., Tribuzio, A.: On the energy scaling behaviour of singular perturbation models with prescribed Dirichlet data involving higher order laminates. arXiv preprint arXiv:2110.15929 (2021)

Rüland, A., Tribuzio, A.: On the energy scaling behaviour of a singularly perturbed Tartar square. Arch. Ration. Mech. Anal. **243**(1), 401–431 (2022)

Rüland, A., Taylor, J.M., Zillinger, C.: Convex integration arising in the modelling of shape-memory alloys: some remarks on rigidity, flexibility and some numerical implementations. J. Nonlinear Sci., pp. 1–48 (2018a)

Rüland, A., Zillinger, C., Zwicknagl, B.: Higher Sobolev regularity of convex integration solutions in elasticity: the Dirichlet problem with affine data in int(K^{lc}). SIAM J. Math. Anal. **50**(4), 3791–3841 (2018b)

Scheffer, V.: Regularity and irregularity of solutions to nonlinear second-order elliptic systems of partial differential-equations and inequalities (1975)

Schwabe, S., Niemann, R., Backen, A., Wolf, D., Damm, C., Walter, T., Seiner, H., Heczko, O., Nielsch, K., Fähler, S.: Building hierarchical martensite. Adv. Funct. Mater. **31**(7), 2005715 (2021)

Tan, S., Huibin, X.: Observations on a CuAlNi single crystal. Contin. Mech. Thermodyn. **2**(4), 241–244 (1990)

Tartar, L.: Some remarks on separately convex functions. In: Microstructure and Phase Transition. Springer, pp. 191–204 (1993)

Winter, M.: An example of microstructure with multiple scales. Eur. J. Appl. Math. **8**(2), 185–207 (1997)